



Application of thermal analysis methods in biology and medicine

JELENA MACAN*

University of Zagreb, Faculty of Chemical Engineering and Technology, Zagreb, Croatia

*Correspondence:

Jelena Macan

E-mail address: jmacan@fkit.hr, jmacan@fkit.unizg.hr

Keywords: differential scanning calorimetry; thermogravimetry; dynamic mechanical analysis; thermomechanical analysis; tissues; plants; animals

List of abbreviations

DETA	– dielectric thermal analysis
DMA	– dynamic mechanical analysis
DMSO	– dimethyl sulfoxide, (CH ₃) ₂ SO
DSC	– differential scanning calorimetry
DTA	– differential thermal analysis
DTG	– derived thermogravimetric
EGA	– evolved gasses analysis
LT ₅₀	– lethal temperature at which 50 % of the organisms die
PVS2	– plant vitrification solution 2
TD	– thermodilatometry
TGA	– thermogravimetry
TMA	– thermomechanical analysis

Received January 4, 2023
Revised March 9, 2023
Accepted March 17, 2023

Abstract

Thermal analysis methods are widely used in the characterization of substances and materials in chemistry and engineering. But they also find their application in life sciences: biology and medicine. This paper exhaustively and critically reviews the application of the most commonly used thermal analysis methods for the characterization of organs and tissues of plants, animals, and humans. The methods are suitable for differentiating between several types of water in a cell, optimizing treatment, storage, or cultivation conditions, following plant or animal development, medical diagnostics and modelling, and more. Expertise developed in the characterization of synthetic materials and molecules can be transferred to that of biological tissues and biomolecules and opens a perspective for interdisciplinary research. Still, researchers should take into consideration the inherent complexity of biological samples, as well as inevitable changes when isolating the tissue from the living organism.

INTRODUCTION

Thermal analysis methods comprise all instrumental methods that measure some property of a material as a function of temperature (or time) when subjected to a controlled temperature program. Although there are now numerous techniques which enable such measurements (e.g., heated microscope stage), the term is usually applied to several established techniques: thermogravimetry (TGA), differential thermal analysis (DTA), differential scanning calorimetry (DSC), thermomechanical analysis (TMA), dynamic mechanical analysis (DMA) thermodilatometry (TD) and dielectric thermal analysis (DETA) (1,2).

These techniques were initially developed for the characterization of polymers and ceramic materials, but with time their use evolved to encompass all sorts of materials and substances, including those of biological origin. For example, DSC is regularly used in the pharmaceutical industry (3,4), while several thermal analysis methods are used in the food processing industry (5–9). Naturally, these methods have also found their use in biology and medicine, so the aim of this paper is to review their historical and current use and hopefully inspire future research.

As the fields of biology and medicine are quite broad, this review will be limited only to the “pure” biological research, excluding the papers dealing with the development of biomaterials and materials for biomedical applications, as well as those researching biomass as a raw material for the production of energy or composite materials, as adsorbents etc.

Also excluded will be the field of biochemistry: the use of DSC to study biological macromolecules and their interactions with each other and with possible pharmaceuticals is widely reported on (10–22), the earliest reviews dating back to 1989 (23). Hansen et al. (24) can be recommended as a good introductory paper for those interested in the topic.

This paper will first give an overview of thermal analysis methods, their working principles and their main applications, as well as the way in which measurement conditions can influence the results and how to control for such influences. The use of thermal analysis in biology will be divided into two sections: plants and animals, followed by the use of thermal analysis in medicine. Most of the research on mammals will be presented in the section on medicine since the animals were model organisms in medicinal research. Finally, general conclusions and prospects will be given.

PRINCIPLES AND APPLICATIONS OF THERMAL ANALYSIS METHODS

Thermogravimetry

Thermogravimetry measures the changes in the mass of the sample with time or temperature under a controlled atmosphere, using a thermobalance (2,25). The atmosphere is most often inert (nitrogen) or oxidative (synthetic air, composed exclusively of 79 % of nitrogen and 21 % of oxygen, with no other components). Other reactive gases such as atmosphere with controlled humidity or CO₂ are also used. A mass loss is usually a result of thermal degradation, but it can also be due to evaporation. More rarely, a mass gain is due to a reaction with the atmosphere or the adsorption of gases from the atmosphere. Residual mass after degradation is often used as a

measure of inorganic content or “ash”. Derivation of the thermogravimetric curve makes the mass losses easier to discern (Figure 1), and sometimes these curves are referred to as DTG curves.

TGA is commonly used to determine the thermal stability of organic substances such as pharmaceuticals or polymers, as well as to help determine the drying conditions and water (moisture) content. It can also be used to quantify known components of the sample by measuring the characteristic mass loss of their degradation (e.g., CaCO₃ content from mass loss due to CO₂ release). To help identify the mass losses, TGA is often used in combination with DTA and DSC, which show whether the change is accompanied by the release or the absorption of energy (exothermic or endothermic change, respectively).

Differential thermal analysis and differential scanning calorimetry

DTA and DSC are differential methods, measuring the difference in signal between the measured sample, which undergoes changes, and the reference sample, which remains unchanged during the measurement (2,25). Both samples undergo the same temperature program, either in the same furnace (DTA) or in two simultaneously heated furnaces (DSC), and the signal is measured as a function of time or temperature. DTA is the older method, measuring the difference in temperature between the samples. If the measured sample undergoes an endothermic change (i.e., absorbing the heat from the environment) its temperature will decrease in comparison with the reference sample, and vice versa: if it undergoes an exothermic change, its temperature will increase. The difference is then plotted as either a positive or a negative deviation from the baseline, so-called endothermic or exothermic peak or maximum.

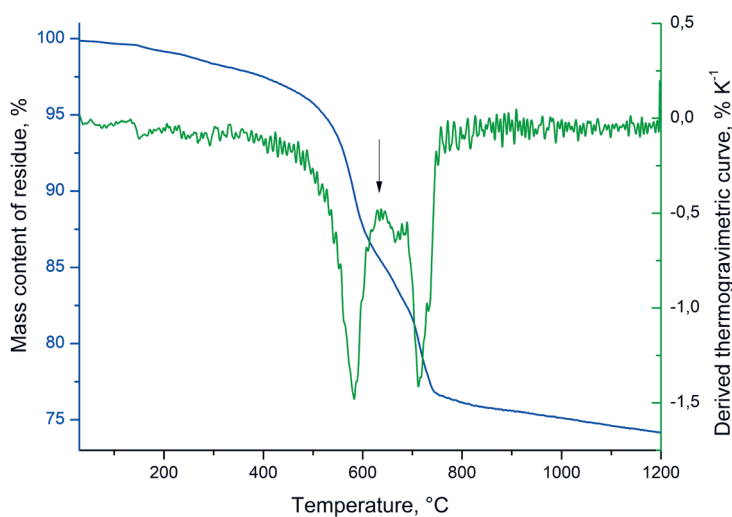


Figure 1. An example of a thermogravimetric curve (blue) and its derivation (green) for a mixed (Ca,Mn)CO₃ carbonate sample. The arrow marks the temperature where the mass loss for one carbonate stops and the other begins.

On the other hand, DSC measures the differences in heat flow, dQ/dt , between the samples: either calculated from the temperature difference between the samples and the furnace or directly from the power needed to keep both samples at the same temperature (22). The resulting curves are very similar to those obtained by DTA but also give quantitative information about the enthalpic effect of the change and the thermal capacity of the sample. Thus, most instruments today are DSC, while DTA is used almost exclusively in coupled techniques such as DTA-TGA or TMA-DTA, where it gives additional information to a quantified change measured by the other method.

Effects measured by DTA and DSC are either phase transitions (crystallization, melting, solid-solid transition, evaporation, sublimation) or reactions (degradation, crosslinking etc.). The temperature of an effect is usually determined from its maximum or onset, as shown in Figure 2., while the enthalpy is determined by integrating the DSC maximum. The DSC instruments are usually calibrated using standards with known temperature and enthalpy of melting, most commonly indium. Correct determination of a baseline for integration can be complex and requires familiarity with the sample and the changes it undergoes. From the experimental enthalpies of melting or evaporation of water and the known molar enthalpies of melting or evaporation, it is possible to quantify the amount of water undergoing the change (26). For example, if the total amount of water in the sample is known, the proportion of frozen water can be calculated from the measured exothermic effect of freezing (27).

DTA and DSC can be used to determine glass transition temperature (25), at which amorphous elastic solid changes from a glassy state into a rubbery or fluid state, depending on whether it is fully chemically crosslinked

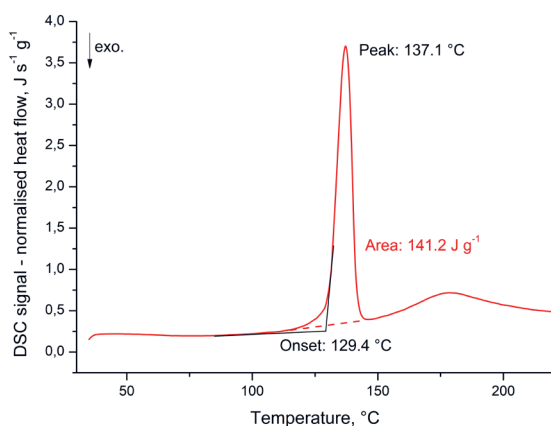


Figure 2. A DSC curve showing the melting of an organic crystal containing zinc. The onset temperature is less sensitive to measurement conditions and sample size than the peak temperature, so it is a better representative of the melting temperature. The area of the endothermic maximum gives the enthalpy of melting.

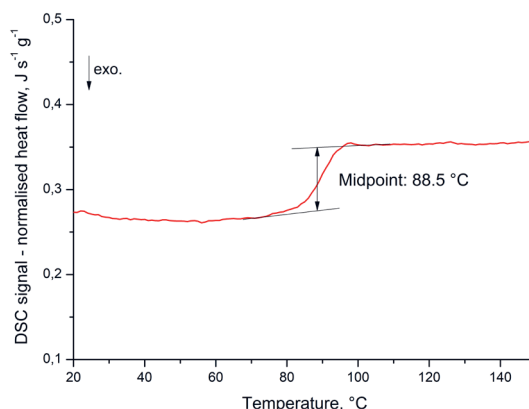


Figure 3. DSC curve of a fully crosslinked epoxy-amine resin, showing a glass transition, its temperature determined from a midpoint of the step.

or not. Unlike the melting of crystals, there is no maximum, but a stepwise shift in the baseline, as shown in Figure 3. A liquid or a rubbery solid can be vitrified, i.e., turned into a glassy state, if cooled fast enough to prevent the formation of crystals. On the other hand, an amorphous glassy solid can crystallize during heating, as its molecules gain enough energy to rearrange into an ordered crystalline state: this phenomenon is called cold crystallization. Polymers may be partly amorphous and partly crystalline since it is difficult for macromolecules to fully crystallize: this type of structure is called semi-crystalline and exhibits both a glass transition step and a melting endotherm in its DSC curve. The presence of small molecules in a macromolecular material can increase the mobility of molecular segments, thus decreasing the glass transition temperature and making the material more flexible: this is called the plasticizing effect, and the molecules are called plasticizers.

Thermodilatometry, thermomechanical and dynamic mechanical analysis

TD, TMA and DMA are based on measuring changes in sample dimension with time and temperature (2,25). In thermodilatometry the sample is under negligible stress, in thermomechanical analysis the stress is constant, and in dynamic mechanical analysis the stress oscillates sinusoidally. The stress can be compressive, tensile, bending or shear stress (28), and the type of applied stress must be stated to enable a correct interpretation of the results.

Thermodilatometry can be linear or volumetric, depending on whether the change in only one dimension (usually length) or all three dimensions is measured. The result is the linear or the volume thermal expansion coefficient (29). A marked change in the coefficient indicates a phase change, a chemical reaction, or sintering of the sample. To make the identification of the change easier, the difference in temperature of the sample and the fur-

nance can be used to calculate an approximate DTA curve. Thermodilatometry can also be performed on TMA instruments using an appropriate probe and negligible compressive stress. As dilatometers were developed for the investigation of ceramic materials, they are optimized for a wider temperature range and for larger samples than the TMA instruments, which were developed for the investigation of polymers.

TMA instruments can have several functions, depending on the shape of the measuring probe (30). The main applications are dilatometric and swelling measurements, determination of phase changes or softening of the material, but compressive or tensile modulus can also be measured. Probes with a sharp tip can be used to measure soft coatings on hard substrates without previously removing them, which is an advantage in comparison to DSC.

DMA instruments are mainly used to determine the viscoelastic properties of the samples, i.e., the proportion of elastic strain and of viscous flow, which are in phase and out of phase with the dynamic oscillatory stress, respectively. The elastic strain is perfectly recoverable after the removal of the stress, while the viscous flow is irreversible. Therefore, the modulus calculated from the in-phase stress is called storage modulus (since the energy “stored” in the deformation can be recovered), while the modulus calculated from the stress 90° out of phase is called loss modulus (since the energy is “lost” in viscous flow) (25,28). The storage modulus is similar to the Young modulus of elasticity, but they cannot be equated unless the material is ideally elastic. Some materials are more elastic and some more viscous, and the ratio of these properties’ changes with measurement conditions and with phase changes in the investigated material. In the case of sinusoidal oscillation, δ is the phase angle by which the stress lags after the strain. The ratio of loss and storage moduli is equal to $\tan \delta$, also called loss tangent or loss factor (25,28). A maximum in $\tan \delta$ can be a measure of the damping (energy dissipating) behavior of the material, which may be important for e.g., amortizing vibrations and shocks in joints (31). On the other hand, a decrease in $\tan \delta$ can indicate crosslinking in the material, making it stiffer and less viscous (32).

DMA measurements are usually performed in one of two modes: changing the temperature while keeping the oscillation frequency constant (a temperature sweep, see Figure 4), or changing the frequency while keeping the temperature constant (a frequency sweep) (25). The two modes are complementary: the transitions in the sample that would happen at lower temperatures appear at higher frequencies, and vice versa. Measurement at different frequencies will shift the temperatures at which transitions happen (33), with the sole exception of melting. A good overview of the DMA technique can be found in (34). Rheometers function very similarly to DMA instruments, but they are optimized to work with liquids, pastes

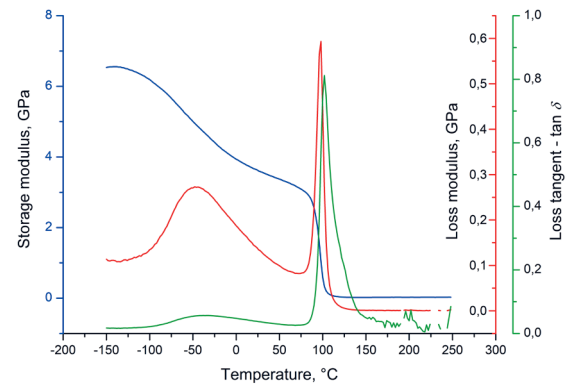


Figure 4. Results of DMA analysis of a fully crosslinked epoxy-amine resin, showing the storage modulus, the loss modulus, and the loss tangent. The maxima at -100 °C are caused by alpha relaxation (glass transition), while those at -50 °C are caused by beta relaxation of side groups.

(highly viscous suspensions of particles in a liquid), gels (lightly crosslinked two-phase materials where crosslinked solid matrix contains the liquid phase) and other soft and mostly fluid samples, so they measure viscosity rather than stress (35,36).

TMA and DMA are also suitable for determining the glass transition temperature, especially in cases where it is hard to discern using DSC (see section *Differential thermal analysis and differential scanning calorimetry*). In TMA, the glass transition is determined from the change in thermal expansion coefficient or from the softening of the material, while in DMA it is determined from the maximum of loss modulus or of $\tan \delta$ curve (the maxima at -100 °C in Figure 4). Since the two maxima are not at the same temperature, it is necessary to state which one was used to determine the glass transition temperature. In case several maxima are present, the most intensive transition (at the highest temperature or the lowest frequency) is called alpha relaxation, the maximum at the second-highest temperature corresponds to beta relaxation, and so on (25,37). The alpha relaxation is usually ascribed to the glass transition, while the beta relaxation is related to the localized motion of small groups of atoms, e.g., a side group. A good explanation of the correlation between the mechanical properties and the glass transition, especially as applied to DMA and TMA, can be found in (38).

Dielectric thermal analysis

DETA measures the electric properties of materials, more precisely how the current flowing through the sample changes as the electrical field oscillates sinusoidally. Resulting are dielectric permittivity and dielectric loss factor, as well as $\tan \delta$ as the ratio of the loss factor and the permittivity (25,39,40). This makes DETA complementary to DMA, as it measures similar changes in mo-

bility within the material. Although it is applicable only for polar materials, often non-polar materials contain enough polar impurities to make the application of DETA feasible. A major application of DETA is the measurement of “ionic viscosity”, a reciprocal value of ionic electric conductivity of the material, to follow the crosslinking of resins beyond the range of rheometers, i.e., when the crosslinking material no longer flows. Therefore, some instruments combine the functionalities of a rheometer with a DETA analyzer.

Influence of measurement parameters

Heating rate and sample mass or dimensions are the most important measurement parameters that should be controlled for. Also influencing the measurements are the atmosphere within the instrument, as well as the crucible or holder used for the sample. To obtain the true properties of a sample, the influence of all these parameters should be accounted for (41). If a series of different samples is to be compared, it is best to keep all the parameters identical, or as close to identical as possible.

The use of small samples/sample masses is one of the main advantages of thermal analysis methods: 1 – 10 mg for DSC and 20 – 50 mg for TGA, while the samples for mechanical analyses can be only a few centimeters in length. Usually, a compromise is made between the intensity of the signal (larger mass) and the sensitivity and resolution of the measurement (smaller mass). Particle size also plays a role (see Figure 5): a small particle size makes achieving and keeping thermal equilibrium easier and decreases the influence of diffusion if a reaction takes place during the measurement. It also exposes the sample more directly to the gases in the furnace.

Most thermal analyses are performed using a constant heating (or cooling) rate. Isothermal measurements (keeping the temperature constant during the measurement) and controlled rate measurements (keeping some change

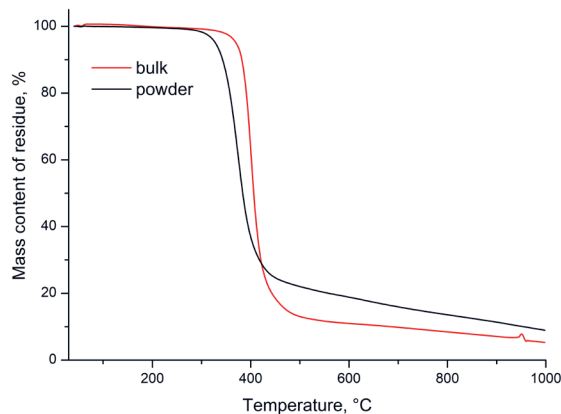


Figure 5. Thermogravimetric curves of fully crosslinked epoxy-amine resin in bulk and in powder form.

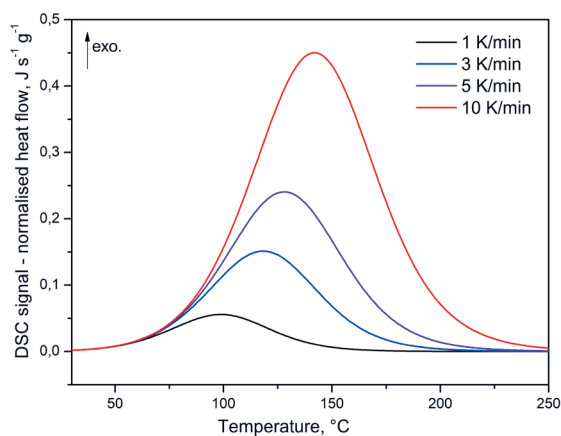


Figure 6. DSC curves of curing epoxy-amine resin at different heating rates, showing the shift to higher temperatures as well as the increase in prominence of the maxima.

in the sample, e.g., a mass loss or a change in length, constant during the measurement) are also performed, but only an occasional example was found when reviewing the use of thermal analysis in biology and medicine. Therefore, only the heat rate will be addressed in more detail. The main limiting factor for the heat rate is avoiding the temperature lag between the sample and the furnace. The lag is most often caused by the size/mass of the sample, as it takes time for heat to be exchanged through the bulk of the sample. Therefore, the methods with small sample sizes, DSC and TGA, can use higher heating rates (most commonly 10–20 K/min), while TMA, DMA and TD rarely use rates above 5 K/min. For kinetic reasons, the effects due to chemical reactions are shifted to higher temperatures when higher heating rates are used (see Figure 6), which may make a comparison of, e.g., degradation temperatures of vascular plants (10 K/min) and algae (20 K/min) difficult (42). Higher heating rates also make effects more prominent but worsen the resolution, so it may be worth it to analyze a sample at several different heating rates to find the most appropriate one.

Although most thermal analysis measurements are performed under controlled heating, controlled cooling is also possible. When cooling to very low temperatures, low cooling rates are required: as a rule of thumb, the minimal temperature achievable when cooling at 10 K/min is ~40 °C higher than the nominal lowest temperature achievable at 2 K/min. Enforced ventilation using simple air compressors enables controlled cooling to ~100 °C at 10 K/min. To reach lower temperatures (~75 °C or even lower), refrigerating units are available, while the quickest cooling and the lowest temperatures (down to ~180 °C) require liquid nitrogen. Refrigerating units require the largest up-front investment but are also the easiest to manage, especially in regular use such as cooling down the instrument between measurements. Liquid nitrogen,

on the other hand, is consumable and slowly evaporates when not used, which increases the operating costs.

Atmosphere type (inert, reactive) can influence the changes the sample undergoes, so most often the inert atmosphere of nitrogen is used. When heating to up to 200 °C air can be regarded as inert for most samples. The composition and flow rate of the gas circulated through the instrument can influence the heat transfer to and from the sample, and so should be kept constant for any series of measurements.

Crucibles in TGA, DTA and DSC influence the measurement through a possible reaction with the sample and through influencing the exchange of heat and gases between the sample and the furnace (43). Obviously, the crucible should not react with the sample in the measurement conditions, nor should it undergo some change itself. For example, single-use aluminum crucibles can be used up to 500 °C, since aluminum melts at 660 °C. Other most common materials for crucibles are alumina (Al₂O₃), steel, copper, and platinum. DSC measurements are most often performed in a sealed crucible, sometimes with a hole in the lid to vent excess gases. TGA measurements, on the other hand, are performed in an open crucible so the gaseous degradation products can be easily removed. Thermal conductivity and heat capacity of the crucibles influences the measurements, but this is compensated for by calibrating the instrument.

Sample holders in TD, TMA and DMA should also be inert and stable in measurement conditions, as well as have mechanical properties which can be compensated for in calibration or safely neglected during the measurement. Unlike crucibles, they are rarely changed once the instrument is purchased. Commonly used materials are quartz glass or steel (for temperatures up to 1100 °C, the glass for greater precision, the steel for greater stress), alumina (up to 1680 °C) and graphite (up to 2000 °C but requiring a vacuum or a non-oxidative atmosphere). Good contact with the instrument probe must be assured for the force to transfer properly, so a variation in the size and shape of the samples, especially the presence of curved surfaces, may result in a large variation of results (44).

For DMA measurements in tensile and bending modes, the sample must be clamped in a holder. This may present problems if the sample is soft or easily deformed, or if the clamping may influence the measured properties. Tendons, for example, have to be completely isolated and clamped using special gummed grips (45), while ligaments may be clamped using the parts of the bone or tooth on which they are naturally fixed (45,46). Sensitive samples such as cuticles can be glued with epoxy to a hard plastic that would serve as the part of the sample to be gripped, but the suitability of the approach should first be verified using an independent sample of known properties, to see if it would influence the results significantly (47).

THERMAL ANALYSIS OF PLANTS

As stated in the introduction, this paper will not include the characterization of plants as raw matter for the production of materials, fuels (biomass) or food. Some borderline cases will be presented as an example of the applicability of thermal analysis methods to the analysis of plants.

Composition and thermal stability of plants

Thermogravimetry is mainly used to quantify various components in plants based on the differences in their degradation temperature. This is not always possible due to essential similarity in the basic chemical composition of organic molecules, which degrade at similar temperatures. The main components of plant matter are cellulose, hemicellulose, and lignin, which all undergo oxidative pyrolysis in the 180–360 °C range, followed by thermal degradation of aromatized char in the 360–540 °C range (41). Some researchers ascribe the maximum at the 340–360 °C range to the combustion of holocellulose (all cellulose species, including hemicellulose), while the peaks and shoulders in the 410–480 °C range are ascribed to the combustion of lignin (26, 42, 48). Hemicellulose usually degrades at a somewhat lower temperature than cellulose, which may be seen as a shoulder in the 280–300 °C range (41, 42). Plant samples also usually show water evaporation up to 120 °C (41). It should be kept in mind that peak and shoulder temperatures are a function of sample mass and heat rate – most of the reported values were obtained at 10 K/min, but other heating rates are also used, and sample masses are rarely reported.

An attempt was made to identify carbohydrate, lipid, and protein content in dry microalgal powder by TGA (49), using characteristic DTG peaks of model compounds. The quantification was impossible due to major peak overlap, but a semi-quantitative evaluation managed to determine which sample contained more lipids or more protein, allowing for relatively rapid screening of desired cultivation conditions. Mineral ash content can be determined easily, if care is taken to select the temperature sufficient for the complete removal of organic components (up to 800 °C) (42), but not high enough to lead to the evaporation of a mineral component, such as chlorine or potassium (49). Differential scanning calorimetry is most often used to quantify the evaporated water or compare enthalpies of combustion (26).

An early work applied the evolved gasses analysis (EGA) on the thermal degradation of lignin (50), a rare example of this method of thermal analysis being applied in biology. Nowadays TGA and EGA are coupled techniques, with simultaneous analysis of the same sample, but in this case the two methods were applied separately. While most sources describe lignin as thermally stable (41), its composition is complex: therefore, it starts to de-



Figure 7. *Miscanthus x giganteus* grown in Germany (53)

compose at lower temperatures, similar to hemicellulose, but due to its aromatic nature the decomposition is spread over a wide temperature range, and parts of it are more thermally stable than cellulose (51).

Other components also influence the thermal stability of plant tissues. Higher content of *p*-coumaric acid increased the thermal stability of miscanthus (Figure 7) stem matter, while the increased presence of ferulic acid led to increased mass loss in the 180–360 °C range (41). Large mineral content (3.8–7.4 % final residue) in miscanthus stem matter shifted cellulose degradation to somewhat lower temperatures, overlapping with the degradation of hemicellulose. Cork thermally decomposes differently from common plant matter, as it is composed mostly of suberin and lignin, with a relatively small content of cellulose (52). Suberin is more resistant to thermal degradation than holocellulose, although less than lignin. The macrostructure of cork also influences its thermal stability and degradation: lenticular channels serve as gas exchange channels.

The applicability of thermal analysis methods for the identification of three types of water in fruit: intercellular (free water), intracellular (loosely bound water) and cell-wall (strongly bound water) was investigated (29). It is very difficult to differentiate between these types of water by TGA since suitable equilibrium conditions are required to separate mass losses during drying. While the removal of free water does not cause shrinkage detectable by TD, the removal of bound water is measurable since it

causes cellular shrinkage and collapse of cells. DSC could differentiate between free and loosely bound water by the change in melting temperature, which will be described in more detail in the section discussing frost tolerance and cryopreservation. TD can measure the expansion of water by freezing, so with the presumption that only the free water will be able to freeze, the bound water can be calculated from the total water content by subtracting the free water as determined by TD. The problem is that the presence of air may strongly influence the results, so not all tissue types are suitable for this measurement (e.g., fruits in general). In any case, the methods are worthy of investigating due to their relative simplicity in comparison with some currently in use.

Mass losses did not significantly depend on different genotypes in the case of the same plant species (41), and there was very little variation in the biochemical composition of the same type of tissues across different species in the same climatic zone (54). Investigation of thermal degradation through the radial profile of several different trees of the same conifer species (55) found that juvenile heartwood (the innermost part of the tree, first grown) was significantly more susceptible to thermal degradation. In conifers, juvenile heartwood contains less cellulose and more hemicellulose and lignin, but it also has thinner cell walls. The authors claimed lignin to be more highly susceptible to degradation than cellulose, which is contrary to the bulk of the research. In this author's opinion, both the macrostructure (i.e., the thinner walls) and the pos-

sible differences in minor components should be regarded as potential causes.

DSC in combination with TGA and infrared spectroscopy was proven useful in discerning between different almond cultivars (56), which mainly differed in their fatty acid composition. The DSC method does not require prior oil extraction, simplifying the procedure. TGA by itself did not show significant differences between the cultivars. DSC can be used to determine the glass transition in seeds, which is weak due to relatively low water content compared to other plant tissues and which may overlap with melting endotherms of fats present in the seed (38). For oil-rich seeds, such as *Citrus* spp. and *Coffea* spp., DSC can be used to distinguish between the phase transitions of lipids and water (57) and drying of seeds makes the thermal effects of lipids much clearer. Identification of the lipids is easily verified by direct comparison with DSC curves of pure extracted oils which show the same transitions. The investigation of three native Australian *Citrus* species (57) has shown that those from a more tropical climate had significantly ($-3\text{ }^{\circ}\text{C}$) higher lipid melt temperature compared to the species from a more moderate climate, due to a larger saturated fat content. The lower lipid melt temperature, i.e., the larger unsaturated fat content, correlated with better seedling recovery after cryopreservation. The variance in saturated and unsaturated fat content in plant oils due to climate is well-known in various species, and the difference is largely genetically based.

Frost tolerance and cryopreservation of plants

DSC and DTA are both especially useful in detecting enthalpy changes due to the freezing of water or melting of ice crystals. The formation of ice crystals is known to damage living tissue, so the temperature at which water in the tissues freezes can be used to judge the frost tolerance of these tissues (58–60), while the disappearance of the freezing effect is widely used in optimizing the pre-treatment of plants for cryopreservation (27,57,61–63). On the other hand, the appearance of a freezing effect during warming is due to the so-called cold crystallization of vitrified (amorphous) water during warming, which can damage the tissue if the sample is thawed too slowly (60). DSC can also be used to follow dehydration during pre-treatment, such as osmotic dehydration (64).

Malyshev et al. (58) have applied the principle of DTA to measuring the freezing temperature of the water inside plant tissues, by attaching one thermocouple to a living piece of tissue, the other thermocouple to a dry, dead counterpart serving as a reference sample, and measuring the difference while both samples were cooled in controlled conditions. The water in live tissues would release heat upon freezing, increasing the temperature of the living tissue in comparison with the dead one. The temperature of this effect corresponded very well to the more

conventionally estimated LT_{50} (the temperature at which 50 % of plants die) while requiring fewer samples and a significantly shorter time. On the other hand, the DTA method must be validated for each new species or organ by comparison with another, more established method. It also has limitations: the investigated plant organ has to be large and robust enough to attach the thermocouple to, and has to contain enough intracellular water to give off a detectable amount of heat. The authors note that most frost-tolerant plants resist frost damage by expelling water from their cells so it would freeze extracellularly. This type of frost tolerance cannot be tested by DTA. The difference in intra- and extracellular water may cause an appearance of a second freezing exotherm: the extracellular water freezes at higher temperatures, while the intracellular water may supercool to a lower temperature, which is when frost damage occurs.

DSC was used to investigate the dehydration and freezing resistance of lichenized fungi (59). Overall freezing exotherm of supercooled water decreased with decreasing temperature, possibly caused by decreased mobility of supercooled water molecules. Since the effects are too low to be detected for a hydration level below 20 %, the measured data was extrapolated to obtain the minimal hydration level at which the ice nucleation still occurs. A similar approach was used when investigating the optimum dehydration level for the cryopreservation of seeds (57).

Investigation of shoot tips cryopreservation (27,61,62) has shown the usefulness of DSC in optimizing the incubation time in PVS2 (plant vitrification solution 2). To avoid freeze damage, prior to exposure to liquid nitrogen for cryopreservation the tissue is partially dehydrated and infused with cryoprotectants (DMSO and ethylene glycol) which promote vitrification instead of freezing, so no ice crystals are formed (61,62). On the other hand, PVS2 components are toxic to tissues, so too long an exposure can outright kill the cells (61,62). DSC investigation can detect the formation of ice, either by measuring the exothermic effect during freezing or the endothermic effect during melting, so the shortest incubation time that still prevents the formation of ice is the optimal incubation time for the future viability of cryopreserved shoots. The DSC can also be used to select the best pre-treatment protocol before the incubation in PVS2 (62). For example, preculture of shoots in trehalose, a specialized sugar which supports low-temperature acclimatization in polar biota and tolerance to partial dehydration in desiccation-tolerant organisms, lowered both the freezing and the glass transition temperature and decreased the melting endotherm, i.e., the amount of ice formed (27).

Decomposition, rot, and carbon sequestration

An interesting application of TGA and DSC is in monitoring the natural decomposition or rot of plant mat-

ter. Reh et al. (26) investigated how the holocellulose and lignin content changed during the decomposition of leaves and needles under field conditions. Interestingly, the heat released per gram of both holocellulose, and lignin changed after the decomposition, indicating the change in their physiochemical properties, not only in their quantity. In general, the mass content of holocellulose decreased, but its enthalpy of combustion increased, while the reverse was true for lignin. The increase in the enthalpy of combustion of holocellulose is ascribed to the concentration of more energy-rich crystalline cellulose in the degradation product, i.e., the energy-poorer hemicellulose degraded, leaving relatively more cellulose as part of holocellulose, and thus increasing the enthalpy of combustion. Thermal and degradation properties of lignin were found to vary significantly between plant species and were thus harder to explain.

Similarly, Ferraz et al. (65) used TGA to characterize the biodegradation of softwood by an ascomycete fungus – the biodegraded wood started to thermally degrade at lower temperatures, due to selective biodegradation of lignin. Alfredsen et al. (66) investigated the applicability of TGA to determine the wood decay by white and brown rot fungi. The results were comparable to chemical analysis in the case of brown rot but not in the case of white rot, where decomposition products modify the lignin structure. Therefore, the applicability of TGA should be verified for each new application. DMA can also be used to study the fungal deterioration of wood (67,68). A correlation between the decrease in modulus and the quantification of fungal DNA (68) as well as mass loss (67) was found. On the other hand, there was little change in the $\tan \delta$ curve shape, indicating that all components of wood were degraded simultaneously (67).

Parameters extracted from TGA and DSC curves were used to model the biochemical composition of unfermented and fermented maize (69). The model has many parameters and has not been tested on an independent sample/dataset, so the wider applicability of this approach remains to be determined, especially since no other researchers have followed this lead.

TGA was also used to estimate the capacity of marine macroalgae and coastal plants for carbon sequestration (42,54), with the presumption that higher temperature of degradation in nitrogen atmosphere (i.e., pyrolysis) corresponds to the overall stability of contained carbon. The validity of this presumption is debatable, as the authors admit (54) since thermal stability does not necessarily correlate with resistance to biodegradation. Plant tissues generally exhibited greater thermal stability than macroalgae, due to the protective effect of their lignocellulose matrix. Variation in mass losses was greater among macroalgal taxa, which possess a greater diversity of cell wall composition and structure and can contain more thermally resistant long-chain fatty acids. In the end, the

prime factor for successful carbon sequestration is the likeliness that the plant or algal matter will be incorporated into sediments, which is more likely for coastal plants than for algae.

Thermomechanical and dynamic mechanical properties

Thermal analysis methods are rarely used to characterize the mechanical properties of plants, as there are more established methods for the determination of modulus of elasticity, such as the three-point bending test. The main advantage of DMA and TMA in comparison with the established testing methods is the ability to measure the viscoelastic properties and to measure them in relation to temperature. Most of the research is focused on the characterization of wood as a construction material and of fruits and seeds as foodstuff. Unlike TGA, in some cases DMA appears to be sensitive enough to differentiate between genotypes/cultivars within the same species (41,70,71).

Plasticizing effect of moisture on plant tissues, especially cellulose (33,72) and starch (73), can significantly influence the results of mechanical testing since dry tissues will be harder and stiffer (74). Thus, the content of moisture should be accounted for or controlled (33,37), which is not always the case. In some cases, DMA measurements are performed on samples submerged in water or other solvents (71). Alternatively, the samples can be wrapped in a sealing film or foil to prevent drying during the measurement (73).

Perhaps the earliest example of the application of DMA to characterize plants is the 1967 paper by Finney (75), who measured the mechanical properties of fruit flesh (apples, pears and peaches) during fruit maturation. The paper cites earlier examples of using vibration to gauge the firmness (ripeness) of fruit. Both pears and peaches softened, i.e., their Young modulus decreased during ripening, but for apples the modulus remained constant, decreasing only when they became over-ripe. The use of DMA in the characterization of fruit texture remains topical, as it was used to characterize six apple cultivars (70). Mechanical properties of the fruit flesh were directly related to those of cell walls, which in turn depended both on microstructure (e.g., apparent microporosity) and composition. Obvious differences in properties between cultivars were found, although with some overlap. Storage modulus (i.e., firmness) decreased with the storage time of the fruit, while $\tan \delta$, correlated with the xylose and hemicellulose compositions, did not change significantly.

Blahovec and Kouřím (76, 77) used DMA and DETA in the characterization of carrots and potatoes. The modulus decreased with the increase in temperature, reportedly due to the denaturation of proteins. The repeatability of results may be poor since the authors chose to give

relative values of moduli. Significant changes in moduli start at $-70\text{ }^{\circ}\text{C}$ and are correlated with the loss of membrane stability, as well as the damage in cell walls accompanied by starch gelatinization and swelling (77). DETA appears to be more sensitive to this change than DMA. Drying pre-treatments were found to decrease the equilibrium modulus of a Chinese medicinal plant root (74), as they disrupt the cell structure – this eases the drying but decreases the mechanical support of the cell walls. The modulus decreased in direct correlation with moisture loss during drying, probably due to increased porosity of the tissues with water removal. In the last stages of drying the tissues hardened again, likely due to the loss of plasticizing effect of moisture.

Horvath et al. (71) have demonstrated the applicability of DMA as a simple static method for testing the modulus of elasticity of young trees, i.e., the samples with small diameters, which are not suitable for the standard methods used on mature wood. Differences in the genetics of trees result in different mechanical properties of wood, so early testing helps to choose the most appropriate genetic line for cultivation. Reduction in lignin quantity was found to be the main reason for the reduction in modulus.

The correlation of mechanical properties of miscanthus stem fragments with the genotype and the position of the fragment (upper or lower part of the stem) was investigated (41). Unusually, the position on the stem had shown no influence on mechanical properties, while the genetic influence was marked. The highest stiffness corresponded to the highest ferulic acid and the lowest *p*-coumaric acid content. Ferulic acid is known to act as a crosslinker for hemicellulose in the cell walls. On the other hand, cellulose and lignin content had shown little influence on the moduli, despite the structural role of these molecules. Thus, the differences in moduli/stiffness cannot be simply ascribed to differences in biochemical composition or the presence of specific components, as their structure doubtlessly plays a significant role (e.g., the increase in the degree of crystallinity will lead to an increase in the modulus).

Mechanical properties of hullless barley stem were investigated by DMA to obtain useful information on harvesting and processing (33). As the mechanical properties of the stems are affected by the stem maturity, size, moisture content and genetic variety, all these parameters have to be considered. DMA investigations of bamboo found two glass transitions which were ascribed to cellulose and lignin, but the transition temperatures differed for different parts of the bamboo (outer or inner wall, e.g.) (72). In this author's opinion, other components of plant tissues besides water should influence the glass transition, so more care and thought should be given to ascribing the causes of the measured effects.

Williams (40) reviewed the applicability of DSC, DMA, and DETA for the determination of glass transi-

tion in seeds, giving a very good analysis of the advantages and shortcomings of the methods. Walters et al. (38,44) used DMA and TMA to characterize seeds in an attempt to correlate the thermal and mechanical properties of the seeds with their deterioration. Detection of the glass transition or the melting points can be used as a quantitative assay of seed health, regardless of if it is a cause of deterioration (due to increased mobility, i.e., decreased viscosity above the glass transition or melting temperature) or its effect. In particular, they used DMA to investigate the embryonic axes of pea and soybean seeds, representing long and short survival times, respectively. The glass transition of the peas was less pronounced and at lower temperatures in comparison with the soybeans, while beta-relaxation maxima due to the mobility of smaller pendent molecular segments were at basically the same temperature for both. Thus, the storage stability of the seeds is more complex than the simple determination of the glass transition, as the molecular mobility persists even below the glass transition temperature, and the complex composition of seeds will likely influence the processes which happen in them during storage. Others applied DMA to characterize rice kernels and oat grains (73,78) and ascribed the observed transition at $-55\text{ }^{\circ}\text{C}$ to glass transition in starch (73).

More detailed analyses of DMA curves are mostly used to characterize wood as a construction material. Relaxation processes in the $-90\text{ }^{\circ}\text{C}$ – $-80\text{ }^{\circ}\text{C}$ range are ascribed to the motion of methyl (79) and methylol (51) groups. Hemicelluloses and lignin are known to have distinct glass transition temperatures (79), for example low-molecular-weight hemicellulose at $-40\text{ }^{\circ}\text{C}$ (79) and the lignin at $110\text{ }^{\circ}\text{C}$ (51), although the temperature ranges in which they occur do largely overlap (37). Hemicellulose is also highly hygroscopic, which contributes to the plasticizing effect of adsorbed moisture, and thus its contribution to the mechanical properties of wood should not be neglected (37). As already mentioned, due to the complexity of composition as well as the differences within and between the species, it is difficult to confidently ascribe effects to certain components of wood (37).

THERMAL ANALYSIS OF ANIMALS

Thermal analysis methods were mostly used to characterize shells, cuticles or silk produced by insects and other invertebrates. Almost all investigations on mammals were done for medicinal research, and some investigations of mammalian tissue of general interest will also be covered in the section on medicine since they are topically similar to the papers from the field of medicine. This leaves only several papers dealing with vertebrates. As was the case for plant tissue, the mechanical properties of the tissues are sensitive to the plasticizing effect of water, so great care should be taken to control the level of hydration during measurements, for example by keeping



Figure 8. Harbour seal and its vibrissae (84)

the samples moist between sheets of wetted paper (80) or measuring fully submerged samples (81).

Rheological properties of the muscle of hake fish (*Merluccius hubbsi*) were investigated by DMA, and the resulting curves showed changes consistent with gelation caused by the denaturation of myosin (82). The viscoelastic properties of the jaws of newborn and adult lesser spotted dogfish *Scyliorhinus canicula* were investigated by DMA to see if the change in diet is reflected in the change of jaw bones (80). There was a significant difference in both moduli and $\tan \delta$, which conforms to the fact that newborns are not able to eat the hard food that adults can.

To estimate how harbor seals track their prey using vibrissae (tactile hairs on their snouts, Figure 8), the mechanical properties of the vibrissae immersed in various solutions were investigated by DMA (83). Regardless of the medium, damping ($\tan \delta$) in vibrissae is very low, since they have to transfer the signal without loss to the nerves in the snout.

Invertebrates

TGA was used to investigate the early mineralization of snail shells of *Biomphalaria glabrata* (85), measuring the mass loss of embryos and egg masses to determine the CaCO_3 content from the characteristic loss due to CO_2 release from carbonate. The required calcium is taken up from the environment, as the calcium and CaCO_3 content in the embryo starts to increase after 72 h of development.

Aldred et al. (86) used DMA in tensile stress to investigate the mechanical properties of mussel byssal threads, with which the mussel anchors itself on the surface. Dried threads showed several yield points, while the hydrated ones usually only showed one, but not all threads gave clear readings. Since the analysis was only performed on those which did, this may influence the relevance of the results.

Mechanical properties of insect cuticles are regularly investigated by DMA. The change in mechanical properties of the forewings (elytra) of two beetle species during maturation (32) confirmed the hypothesis that the outermost layers mature first and harden by a combination of crosslinking (evidenced by the decrease in $\tan \delta$) and a less significant contribution of dehydration (decrease in the plasticizing effect of water). No change of storage modulus and $\tan \delta$ with maturation was seen in beetles where the expression of a cuticular protein was suppressed, indicating that this protein plays a role in the crosslinking process. As cuticle tanning in insects usually goes together with hardening, the correlation between the color of the elytra of *Tribolium castaneum* beetle and their mechanical properties was investigated (47). No significant difference was found between variously pigmented mutants and the wild strain, except for completely black elytra which had an increased $\tan \delta$, indicating a less cross-linked structure, which the authors connected to metabolic changes. As samples are usually not tested fresh, an investigation of the influence of preservation

treatment on the properties of insect cuticle (locust hind leg) has shown that freezing at -20°C preserves properties the best (81).

Silk from domesticated silkworm *Bombyx mori* and wild *Philosamia ricini* was investigated by TGA and DSC (87). *B. mori* silk degraded in one step, while *P. ricini* silk degraded in several steps, and this difference persisted even after the removal of sericin (binding protein) from the silk. The silk of a wild silk moth *Gonometa postica* reared either indoors or outdoors was investigated to judge the viability of indoor rearing (88). The rearing conditions were found to influence the property of silk, possibly due to the shorter life cycle of the larvae raised indoors, but not its thermogravimetric profile.

Porter et al. (89) suggested a model for predicting the thermomechanical properties of spider silk, which is more evenly spun and thus has more homogeneous properties than silk-worm silk. They connected the chemical composition and semicrystalline (part crystalline, part amorphous) structure of the silk with its properties and ascribed the relaxation maximum at $\sim 200^{\circ}\text{C}$ to amide segment interactions. Blackledge et al. (90) investigated the silk of a cobweb-weaving black widow spider *Latrodectus hesperus* by continuous dynamic analysis, a variant of DMA that allows for greater extension in the sample. Both storage and loss moduli showed significant changes in trend at the yield point. This is in line with the semicrystalline polymer molecular model of silk: the hydrogen bonds in the amorphous part fail at the yield point, allowing the polymer chains to start to align, increasing the moduli. Sticky regions of the silk fibers had lower initial storage modulus and higher initial loss modulus but did not show the drop the others did – this is due to higher levels of hydration, which disrupt the hydrogen bonds.

Of particular interest may be the work of Motokawa, who used DMA to investigate echinoderm body walls, from sea cucumbers (91) to starfish (92), and proposed a molecular model to explain the observed behavior. Echinoderms have collagenous connective tissue which can rapidly alter its mechanical properties, so-called catch or mutable connective tissue. Testing was done in a self-assembled instrument on samples submerged in artificial seawater. Soft-state samples were stored and tested in calcium-free water, while the stiff state was achieved by various chemical and physical stimuli and was found to be reversible. Both elasticity and viscosity (i.e., both storage and loss moduli) changed as the states changed. The mechanical properties of stiff states did not depend on the kind of stimuli that caused the stiff state.

Unicellular organisms

As mentioned, DSC is often used to characterize different biomolecules, which is beyond the scope of this paper. But it can also be applied to whole cells of unicellular organisms. The standard procedure includes the use

of hermetically sealed pans to avoid evaporation of water during the measurement (93–98), a rescan to determine the reversibility of changes and help draw the baseline (94), as well as using suspension buffer (95) or water (93,96–98) as a reference sample. The mass of the reference sample is usually approximately equal to the expected mass of water in the sample (96), and the correction can be further adjusted when the true water content is determined after DSC measurement (98). Reversible changes that are noticed are mostly due to the melting of DNA (94,96,97).

Miles et al. (94) presented one of the earliest applications of DSC for the investigation of the thermal resistance of a range of microorganisms, connecting the resistance as determined by DSC to the death rate of microorganisms exposed to heat. They were also the only ones to stress the need to control the results for the inevitable contamination with the substrate, but agar was found to show no discernible DSC effects and its influence could safely be neglected. Although variable, DSC curves showed some commonalities in the size and position of endothermic maxima which allowed for their assignment. The onset of thermal denaturation was determined from the inflection point of the most intense maximum appearing at -70°C , but there was no common feature associated with the maximum death rate of the microorganisms. The temperatures of the onset and maxima shifted to significantly higher temperatures in the case of thermophile bacteria. Soon after that, the largest endothermic effect was ascribed to the denaturation of the ribosome (97, 99), even in archaea (96), and DSC was found to be a useful method for measuring its denaturation in whole-cell analysis (99). It is considered good practice to confirm this assignment by isolating the ribosomes and analyzing them by DSC separately (95–97). Usually, there is little difference in the DSC curves of whole cells and of the isolated ribosomes.

DSC was used to determine the heat inactivation of *Escherichia coli* and *Lactobacillus plantarum*, and a correlation between the enthalpy of denaturation and the viability of cells was found (97). Survivability of *E. coli* was also determined after the thermal treatment in DSC (98), as a quicker alternative to growing cells in culture after isothermal heat treatment but requiring very careful data collection and analysis. The addition of salt was found to influence the thermal stability of *Listeria monocytogenes*, shifting the denaturation maximum of the ribosome to higher temperatures for the largest salt concentration (95). DSC was also used to evaluate high hydrostatic pressure treatment for sterilizing perishable foods without using heat. The sensitivity of *Staphylococcus aureus* and *E. coli* to the treatment was determined by measuring the total enthalpy change and thermal stability of the treated and untreated bacteria (93). The maximum at -70°C attributed to the denaturation of ribo-

somes decreased after the treatment, indicating successful sterilization.

Thermal stability and glass transition in bacterial spores are also commonly investigated by DSC. DSC curves of *Bacillus megaterium* spores were analyzed and maxima were assigned with the help of DSC curves of a decoated spore and spores in various states of germination (100), in an attempt to link the effects with the inactivation and killing temperatures of the spores. As the authors note, denaturation of one key molecule may be enough to kill a spore, and yet not be detectable by DSC which gives the overlap of all the processes happening at the same temperature. Glass transition in spores can be tied to their heat resistance, similar to the rationale of seed storage lifetime already described in section Thermomechanical and dynamic mechanical properties of plants. Therefore, the glassy state of *Bacillus subtilis* spores was investigated by DSC in an attempt to find the reasons for their heat resistance (101). Previous research reported glass transition of highly desiccated biopolymers, such as those present in the spores, to be difficult to detect by DSC. The authors only managed to detect a transition in the 90–115 °C range after all the water present had evaporated in a preliminary scan using non-sealed pans. The transition was also found in decoated spores and extracted membrane material, but unfortunately the authors did not attempt to quantify the step and so conclude which spore component contributes and in what amount. Spores of *B. subtilis* and *B. cereus* were also investigated in hermetically sealed pans, to see whether the endothermic transition reported at ~50 °C and linked to the coat can be attributed to a glassy state (102). The findings were too indeterminate, unable to differentiate between various biopolymers and highly influenced by e.g., the water content. Still, it is refreshing to see “inconclusive” results being published – a negative result is still a result, and not appreciated enough in science publishing.

Illmer et al. (103), improving on work by Uribebarrea et al. (104), suggested a facile thermogravimetric method to distinguish between extracellular and intracellular water in unicellular organisms, by using infrared balance to heat the samples and record how the mass decreases with time. Minima in the second derivation of the mass loss curves are an indication of a barrier that needs to be broken for intracellular water to start to evaporate. The presence of two such minima for yeast, a eucaryote, compared to one for a prokaryote, indicates a possibility to differentiate between distinct types of intracellular water in more complex eucaryote cells.

THERMAL ANALYSIS IN MEDICINE

As mentioned previously, a substantial portion of the research presented here was performed on mammals as model organisms and could thus easily be applied to biology. After some examples of the earliest applications, the

subject matter is divided according to the type of tissue investigated.

Application of DMA in medicine goes back to the very beginnings of the method, as from 1968 on, Apter et al. (105) applied it to the study of biological tissues. In the cited paper, they investigated the urethral tubes of dogs and calves and applied an idealized physical model in an attempt to clarify the effects observed by DMA. No anisotropy in muscle direction was found, so most of the studies were carried out in longitudinally cut muscle. The storage time influenced the results since muscles first went into a spasm and then relaxed with time. Due to the recontracting action of the strained muscle, instead of phase lag for viscous behavior, a phase “lead” was seen. This behavior stopped after the tissue died. An interesting example of the early use of DMA is Fitzgerald’s attempt to determine life-to-death transition in various human and animal tissues (106). He found that both storage compliance (reciprocally proportional to modulus) and $\tan \delta$ decreased with time post-mortem until they reached a stationary state approximately 5–6 hours post-mortem. This state persisted until the onset of decomposition.

Both works underline a variable in tissue investigation which is not usually significant for the characterization of materials: time since the sampling, which is most often time post-mortem. Dying of the tissue is a process that starts with sampling and should either be accounted for by controlling the time it takes from sampling to analysis or stopped by various preservation methods. Viscoelastic properties of the tissues can change significantly with time post-mortem (107), for example decreasing the stiffness (108). On the other hand, sometimes the time post-mortem does not have a significant influence (109). If the tissue is preserved, it should be verified whether the preservation procedure influences the properties of the tissue. Freezing, for example, was found to cause some disintegration in the eye lens (110).

To prevent drying out during DMA and TMA measurements, samples should be kept wet (45, 111, 112) or submerged (46, 106, 113, 114) during measurement. Care should be taken to avoid over-moisturizing which may lead to swelling (112). Oil (usually silicon oil) can be used as an evaporation blocker during measurements (39, 110). Some authors measure DMA in frequency ranges characteristic of physiological conditions under which the tissue functions in the living organism: from the movement of joints (115) to heartbeat (34) and blink frequency (116).

Bones and cartilage

As early as 1978, Aoba et al. (117) used DTA/TGA to investigate mineral tissue of a tumor excised from a patient’s mandible to compare it to that of bone and teeth. Central tissue was quite similar to that of the bone, while peripheral tissue contained more organic connective tissue. Otherwise, when researching bones and cartilage

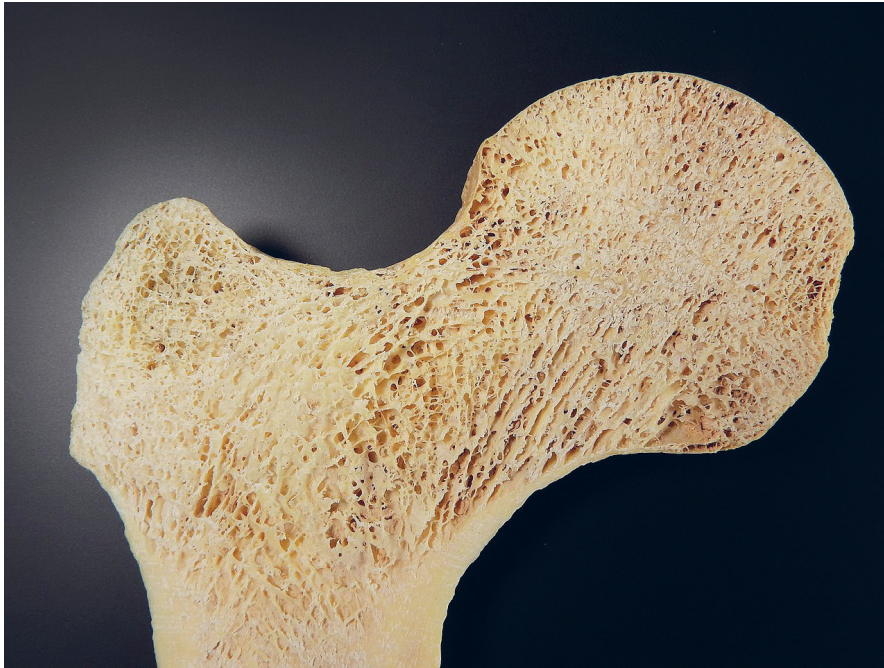


Figure 9. The porous structure of human femoral bone from the anthropological collections of the Department of Biology and Environmental Studies of the Faculty of Education of Charles University in Prague (124)

DMA is the most often used thermal analysis method, since both the bone and the cartilage are viscoelastic materials (115) whose mechanical properties are of interest. Osteochondral tissue (combined bone-cartilage structures) of leg joints drew the most attention of the researchers, since joint deterioration with age is one of the more prominent medicinal problems, and DMA enables investigations at physiological frequencies which should be representative of *in vivo* joint and bone behavior (115).

Testing bone and cartilage as one unit is important since the health of one influences the health of the other. Therefore, dynamic mechanical behavior of bovine cartilage, bone and osteochondral cores containing both the bone and the cartilage was investigated (115). A correlation between bone morphology and viscoelastic properties of corresponding cartilage was found, showing that bone and cartilage interact and influence each other in ways as yet unknown. Higher bone mass density correlated with higher loss modulus in cartilage. Variation of loss moduli with the increase in frequency differed for different tissues: for bones it decreased, for cartilage it increased, while for cores it remained mostly frequency independent, due to cancelling effect of bone and cartilage contributions. Maybe that property serves to preserve joint homeostasis and prevent damage in use.

A similar analysis of human osteochondral tissue obtained during hip replacement surgeries also found that the viscoelastic properties of a bone-cartilage unit differed from those of separate tissues (118). Contrary to (115) the behavior of storage modulus varied, which may be due to

differences in species or joint location (knee vs hip). The authors stress the importance of interaction and interphase on joint properties, especially for energy transfer during stress.

Espino et al. (119–121) first confirmed the suitability of bovine cartilage to model human cartilage and then investigated the differences depending on location (femoral or tibial) and thickness using DMA. They found that thicker parts have lower moduli, so the proportion of stored and dissipated energy does not change across the joint (120). As articular cartilage contains ~70 % of water by weight, its plasticizing effect is significant. Storage stiffness thus increased with dehydration up to a point and then decreased again, while loss stiffness decreased with dehydration (121). Storage and loss stiffness were both lower when measured on a substrate with lower bone density. Since the substrate was not the original bone the cartilage was attached to, it is questionable how much of the variation is a measurement artefact (121).

Mechanical properties of cancellous (porous, Figure 9) bovine femurs were investigated by DMA (122). Surprisingly, there was no clear correlation between the density (i.e., porosity) of the bone and its modulus, due to the complex macrostructure of trabeculae within the specimens. The authors successfully modelled the relaxation modulus of the bone. The damping behavior of bovine rib bones was investigated using DMA, DSC and TGA, the latter two of which were used to determine the water content and so account for its plasticizing effect (123). The amount of water determined from DSC maxima of melt-

ing and evaporation of water was in reasonable agreement with the mass loss during evaporation as determined by TGA. The first DMA damping ($\tan \delta$) maximum at $\sim 50^\circ\text{C}$ corresponds with the denaturation of protein and melting of fats visible in DSC, but the subsequent loss of water and other fluids decreases the damping behavior. The second damping maximum is at different temperatures for cancellous and cortical bone, due to the differences in their structure.

The structure and composition of bones can be influenced by diet, ageing and medical treatments. The influence of calcium deficiency in food on the bones of growing rats was investigated using TGA to determine the inorganic content of the bones (125). The bones of rats with calcium deficiency contained less inorganic matter, and the weight loss of organic components in the 200–600 $^\circ\text{C}$ range was more pronounced. The effect of ovariectomy (i.e., estrogen depletion, simulated menopause) on the elastic properties of sheep (126) and rat (111) bones was investigated by DMA. Namely, the bone density determinations are not good enough predictor of fracture resistance of the bone, presumably due to a significant contribution of the parts of bone not visible by X-ray, i.e., the organic components. No significant changes in moduli and $\tan \delta$ were observed in the case of rat bones, although significant differences were found by other methods of mechanical testing (111). For sheep bones, a change could be observed and was especially marked in $\tan \delta$ decrease, significantly decreasing the damping (energy dissipating) ability of the bones (126). The influence of diclofenac treatment (known to deteriorate bone structure) and exercise on female mice bones was also investigated by DMA (127), but the results were mostly ambivalent, with no major statistical differences. This is not unusual for mechanical property testing, where a large number of measurements is needed to obtain satisfactory statistical analysis, which is not always feasible for long DMA measurements.

Investigation of the mechanical properties of human menisci by DMA in compression found that anterior parts had better damping properties, while the mid-body parts had the highest modulus (31). Both moduli and damping ($\tan \delta$) were higher for menisci from male subjects, the stiffness increased with age, and the increase in body mass index (body mass divided by squared height) was associated with a decrease in modulus, maybe as a consequence of increased wear. An investigation of menisci in shear also considered their anisotropy and composition: moduli were higher in circumferential direction compared to axial, and expectedly the moduli increased as the content of water decreased (114).

Rat menisci have visually obvious differences in anterior and posterior horns, as the posterior ones contain more cells and organic components, while the anterior ones are more calcified, heavier, and thicker. The menisci were char-

acterized by TMA to measure thermodilatometric behavior (under negligible load) and dynamic behavior (under cyclic load) (113). Expectedly, the anterior horn was much stiffer in the response to dynamic load, which corresponds with the way the knee is stressed during locomotion. Thermodilatometric behavior of both horns was similar until 73 $^\circ\text{C}$ (presumably denaturation of collagen), when the posterior dramatically expanded, while the anterior expanded only slightly due to high calcification.

Cartilage tissue can be used in cosmetic surgery, for which it can be reshaped using lasers. To see whether such reshaping damages the tissue, cartilage was investigated by DSC (128) and DMA (129). There was some shift in the characteristic phase-transition temperature, but that was deemed insignificant (128). Modulus decreased during measurement due to even a small loss in moisture, and the direction of sampling (transversal or longitudinal) played a part as well, but the ratio of those moduli remained constant and can be considered to be a characteristic of the cartilage (129). The transition temperature of cartilage was in the 50–65 $^\circ\text{C}$ range, similar to that found by DSC.

The optimal freezing and thawing cycle for cryopreservation of articular cartilage was investigated by DSC, to find the conditions that do not lead to ice crystal formation (130). The paper gives a detailed discussion of the steps necessary to bring this to successful practice.

Teeth

Dentists were quick to investigate teeth by TGA: in 1970 Holager (131) published his work investigating enamel and dentin. In both types of tissue, he found and quantified losses ascribed to water, protein (i.e., collagen) centered at roughly 300 $^\circ\text{C}$, and an unidentified carbonate at roughly 700 $^\circ\text{C}$. As 700 $^\circ\text{C}$ is too low to degrade CaCO_3 , he suspected it could be a double salt of MgCO_3 and CaCO_3 , but now we know it was carbonated apatite (132). Losses ascribed to protein were significantly larger in dentin than in enamel, which was mostly mineral in composition. Analysis of dentin by TGA followed in 1972 and found that the water is released up to 200 $^\circ\text{C}$ since it was strongly bound in collagen, while the collagen degradation temperature of $\sim 300^\circ\text{C}$ is much higher than needed for degradation of free collagen, due to the protective action of the inorganic phase (132). The carbonate degrades in the 500–700 $^\circ\text{C}$ range, while the final mass loss with the maximum at 815 $^\circ\text{C}$ is ascribed to the transformation of hydroxyapatite to δ -tricalcium phosphate, with the accompanying release of water.

Similar results were found when investigating dentin by simultaneous DSC/TGA (133). Three mass losses were evident; water removal up to 105 $^\circ\text{C}$, organic matter (collagen) oxidation in the 300–500 $^\circ\text{C}$ range and finally the decomposition of carbonates at $\sim 800^\circ\text{C}$. Etched dentin degraded much the same, only the mineral component

was reduced, and the decomposition of the organic matter started at lower temperatures, 250 °C, confirming the protective effect of the inorganic phase. Carbonate content was determined from the mass loss near 850 °C, while phosphates were assumed to be the final residue after degradation.

Sound and carious enamel and dentin were compared using TGA among other methods (134). Carious dentin had an additional mass loss ascribed to organic components, possibly due to the presence of invading microorganisms or a change in properties of tooth protein due to caries. No decomposition of carbonate was detected in the carious dentin, indicating that it was degraded in the carious processes. The inorganic phase of hereditary opalescent dentin, *Dentinogenesis imperfecta*, was investigated by TGA (135), the organic component previously being digested by collagenase. The mass loss was greater in opalescent than in healthy dentin, probably due to the presence of a poorly crystallized phase containing bound water, which was released upon heating and crystallization.

It is not always easy to source suitable teeth for research, so human enamel and dentin were compared to those of bovine, porcine and ovine teeth, using TGA among other methods (136). Human enamel was the most highly mineralized and the most similar to hydroxyapatite, while bovine dentin and enamel were the most similar to human ones and hence the best candidates to replace human teeth in research.

Connective tissue and skin

TMA was used as early as 1971 to analyze rat and human stratum corneum (the dead surface layer of skin) (30, 137), as well as in combination with DSC to investigate the human stratum corneum (138). Several softening transitions were found: lipid melting and protein side-chain motion (50 °C), change in protein organization (150 °C) and degradation (260 °C). The second transition is sensitive to various alterations of the skin (caused by disease or chemical agents), which indicates a possible alteration in the organization of keratin. The same research group applied DMA to rat and human stratum corneum (139) and found very complex behavior in the physiological range of temperatures (−20 – 60 °C), likely due to melting of water at −0 °C and lipids at −40 °C. DSC investigation of skin from the hands of diabetic and non-diabetic women showed the increased heat of collagen denaturation in the diabetic skin (140), which was ascribed to increased collagen stability due to glucose-mediated crosslinking, but the exact nature of these crosslinks is not known.

DMA was used to investigate rabbit Achilles' tendons and anterior cruciate ligament, both of which are dense tissue composed of collagen, elastin, and proteoglycans (45). Both tendons and ligaments showed a transition from the rubbery to the glassy state as the loads increased,

but a higher load was necessary for this transition in the case of the ligaments. At low load, the main strain is carried by the proteoglycan matrix, while at high strain most of the collagen fibers are fully extended and bear the most load. Thus, the differences in composition and structure (how the components are distributed and oriented in the tissue) will influence the properties of the tissue.

Viscoelastic properties of the human periodontal ligament (connecting tooth root to the jaw) were investigated by DMA (46), to find out how it behaves during chewing and in accidents. Differences with previously reported results on cow and swine ligaments were found, and the location of the ligament on the tooth also influenced the properties of this inhomogeneous tissue.

Internal organs

A major part of the research on soft tissue is focused either on diagnostic applications or on obtaining parameters for modelling the investigated tissue (141–143) to avoid future experimentation on human or animal subjects. Mechanical properties are of particular interest when investigating impact injuries, which seem to do more damage to solid organs such as the liver and the spleen, as well as for modelling the organs in incident simulations (107) and choosing appropriate implant biomaterials (i.e., to match the mechanical properties of the original tissue) (108,143,144).

In 1969, Fallenstein et al. (145) used DMA to investigate brain tissue (white matter) in shear at 37 °C, to model the impact of head injuries on the brain. The brain tissue was found to have high internal damping ($\tan \delta$). A corresponding investigation was performed *in vivo* on rhesus monkeys using an impedance probe, and the influence of blood pressure on the mechanical properties was found, which correlated well with that of autopsied tissue which had no blood pressure. DSC analysis of brain matter of Alzheimer's disease patients in comparison with those of non-afflicted elderly showed lower thermal stability for some afflicted parts of the brain but no difference for others (146), indicating that DSC analysis cannot fully reflect the distribution of neuropathological changes. The detected effects can be ascribed mostly to loss of water which is indicative of tissue tightness and membrane stability.

Mechanical properties of the spinal cord and the brain in rats were investigated by DMA to find suitable biomaterials for tissue repair (108). Differences in loss and storage modulus were found depending on the location in both the spinal cord and the brain, indicating that biomaterials with different mechanical properties may be required to repair them. Porcine brain tissue was also investigated by DMA (143). The authors used mixed grey-white matter, but they commented on the complex composition of the tissue and that further analysis of separate matter should be done since computer models nowadays routinely simulate separate tissues.

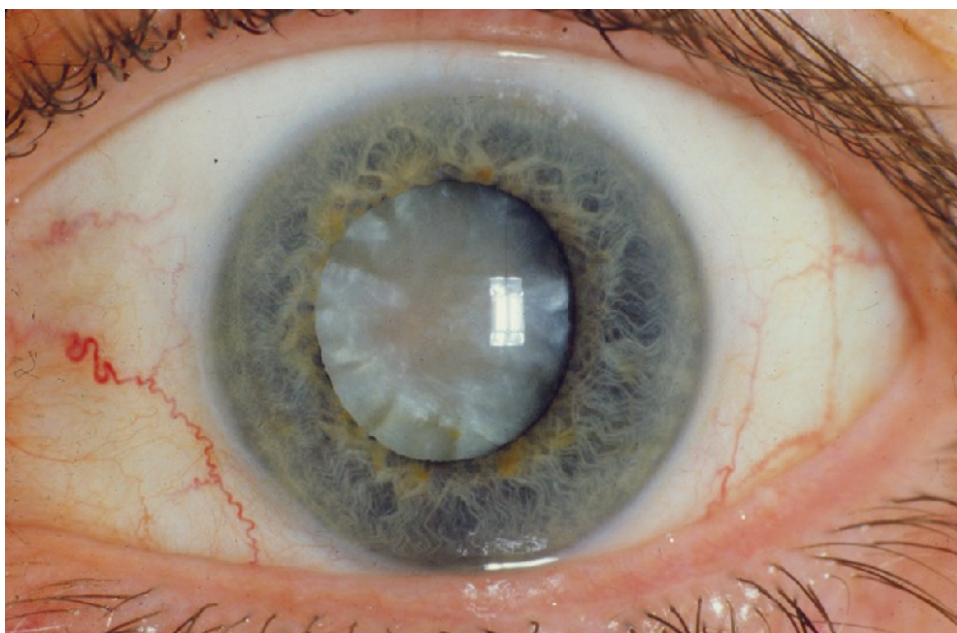


Figure 10. Age-related cataract (154)

Mechanical properties of the human ulnar nerve obtained from the elbows of cadavers were investigated by DMA (147). The difference in storage moduli of proximal (closer to elbow) and distal (closer to hand) nerves was found, but not in loss moduli. Unfortunately, the results may be influenced by the fact that the cadavers were embalmed.

DMA was used to verify *in vivo* mechanical characterization of the liver by ultrasound elastography (107,148,149), by comparing it to *in vitro* post-mortem experiments on the same liver by DMA in shear. In the case of the porcine liver (107), the methods were found to be comparable: the liver acted as a homogeneous, isotropic and mostly elastic body. No influence of cutting direction on liver properties was found, but the researchers avoided the parts with major blood vessels when sampling. The usefulness of ultrasound elastography in diagnosing non-alcoholic fatty liver disease was investigated in comparison with DMA, using rats as the model animal (148,149). Fat accumulation changes the mechanical properties of the liver, which can be seen in both the storage and the loss modulus. While DMA was found to correctly detect the disease, the ultrasound elastography was less successful, possibly due to differences in measurement frequencies. Shear wave elastography for the diagnosis of kidneys was also validated by comparing the results with DMA measurements of the outer cortex of sheep kidneys (150). Blood perfusion of the kidneys probably influences the results, as it could not be mimicked *in vitro*.

The mechanical properties of three parts of the porcine stomach were investigated by DMA (112). The moduli for the three parts differed significantly in the longitudinal

direction but did not differ in the circumferential direction. Some findings conflicted with previous research, underlying again the complexity of investigating biological systems.

Eyes

Thermal analysis methods have been extensively used in the investigation of eye lenses and other eye parts. Bettelheim et al. (151,152) have worked on the topic for two decades, analyzing the melting maxima of water in the lens by DSC. Cataractous human lenses (151) usually have complex endotherms with two melting points, while healthy lenses only show one. The authors ascribe the formation of cataracts to syneresis, i.e., the expulsion of water from the protein network, which results in two domains with differing refraction indices: the denser protein and the watery vacuole. From the difference between the freezable water content (as determined by DSC) and the total water content (as determined by drying) the quantity of tightly bound water which does not freeze could be determined, and it was higher in the healthy lens. Cross-species investigation of water content in the lens was investigated in the same manner (153). The avian lens had the largest water content, likely due to the difference in the type of crystallin and the high content of glycogen.

DMA investigation of the stiffness of human cataract lenses (known to be stiffer than the healthy ones, Figure 10) found the stiffness to be a function both of patient age and the type of cataract, nuclear cataract lenses being stiffer than cortical cataract ones (155). But healthy human lenses were also found to get stiffer (156) with age, so the difference between healthy and cataract lenses de-

creases in older patients. A corresponding investigation of the lenses in shear also found that they become less viscous (i.e., stiffer) with age (110), but uncertainty remains about how much of that is due to cataract formation (157).

The DSC investigation of the influence of pressure on the monkey and the bovine vitreous found that the increased hydrostatic pressure leads to syneresis, i.e., the increase in the content of freezable water compared to the bound water, although the increase was not statistically significant and is probably reversible (152). Storage and loss moduli of the human vitreous body were both found to decrease very significantly with age (109). Rheological investigation of bovine vitreous has shown that it behaves as a lightly crosslinked gel (158).

Mechanical properties of ocular tissues of mice and swine were investigated by DMA so that a future implant material for retinal replacement could match them which would improve its biocompatibility (144). No influence of age was found, but retinal degradation did lead to a decrease in the modulus. The retina is notoriously sensitive and difficult to properly mechanically analyze, due to problems of fixing it into the testing assembly. DMA measurement in compression both simplifies that problem and better reproduces the type of mechanical stress eye tissues would be exposed to *in vivo*. Still, the complexity and anisotropy of tissues such as the retina make a direct comparison with polymeric biomaterials difficult.

DMA was also used to investigate the mechanical properties of porcine lacrimal canaliculus, which drains the tear film from the eye (116). As the probable drainage mechanism is blink-interblink compression and expansion of the canaliculi, viscoelastic properties of such tissues are of interest. Canaliculi were cut open to form a sheet since their size and shape made them difficult to investigate as-is. This raises the question of how well the measurement conditions reflect the working conditions *in vivo*, despite frequencies being chosen to simulate those of a blink.

Veins and blood

Biomechanical properties of different types of leg veins used for arterial reconstruction were investigated by DMA (159). The proportion of elastin to collagen seemed to be the most important predictor of the viscoelastic properties of vein tissue. Varicose veins had the highest content of elastin, as well as more collagen I, which expectedly resulted in the highest modulus (i.e., the highest stiffness) since collagen I is known to increase stiffness. As the varicose veins are much stiffer than arteries, they are not as suitable for grafts as other veins. The femoral veins would be the most suitable, but they are unfortunately less available than the surface (saphenous) veins. The saphenous vein was also found to be stiffer than the internal thoracic artery/mammary artery (which branch-

es from the neck and continues into the thoracic cavity), which is also used as graft tissue (142).

DMA was used to determine the Young modulus of veins in patients undergoing dialysis via an arteriovenous fistula in an attempt to correlate the success of fistula "maturation" (i.e. allowing large enough blood flow) with the mechanical properties of the veins (160). Younger patients had higher moduli of veins, contrary to the usual "hardening with age" expectation, but these were also correlated with fistula failure (although the failure was due to thrombosis, and not a mechanical failure or a failure to mature). The difference in moduli may be a consequence of a previously existing condition, but again the underlying complexity of structures and the selective testing prevents drawing fuller conclusions.

The effect of parameters of freezing/cryopreservation on the thermal expansion of rabbit aorta was investigated by TMA, as it would influence the likelihood of fracture during either preservation or implant surgery (161). As expected, the increased content of DMSO as a cryoprotective agent decreased the stress during the freezing, but for unclear reasons so did the decrease in freezing rate. This was in alignment with the experimentally well-known fact that, to ensure the survival of the tissue, the cooling should be neither too slow (else the ice crystals would form) nor too fast.

Rheological investigation of whole blood and platelet-depleted plasma found that the presence of bacterial lipopolysaccharides may cause anomalous blood clotting (162). Kinetics of clot formation were investigated using rheometry and DETA (39) and it was found that red blood cells decreased clot stiffness, while the increase in fibrinogen increased the clot stiffness and accelerated the clot formation. An investigation of the mechanical strength of platelet clots as a function of storage time and the temperature has shown that clots exhibited gel-like behavior, as would be expected of polymerized cross-linked fibrin (163). Cold-stored platelets formed stronger clots, comparable in strength to those from fresh blood and several times stronger than those from blood stored at room temperature. The authors therefore suggest cold storage as more suitable for transfusions of trauma victims whose blood needs emergency clotting to stop the bleeding. Cold storage is also more convenient overall as it prevents platelet spoilage. Mechanical properties of human fibrinous thrombus samples were also investigated as a part of *in vitro* aneurysm pressure studies, in the frequency range that matched the human heartbeat (34).

The superficial layer of the human atherosclerotic plaques, which is the one to detach and cause heart attacks, was investigated by DMA (164). As stiffness expectedly increased with frequency, stiffer plaques may start to accumulate additional stress when the heart rate increases, leading to rupture and subsequent heart attack (although such occurrences are rare in medical practice).

Other bodily fluids

In a highly interesting paper, Chagovetz et al. (165) have shown that DSC can be used as a screening tool to identify glioblastoma multiforme tumor from concentrated samples of cerebrospinal fluid, as the melting temperature of the fluid was shifted by 5 °C in comparison to that without the glioblastoma. DSC was also used to analyze bovine meibomian lipid, a component of the tear-film lipid layer on the eye (36). Both freezing and evaporation of water could be identified, and water content could be calculated from the enthalpies. The melting of the lipid component could be identified as well, but DSC was unable to differentiate between three lipid phases which melt at similar temperatures. The similarity of the melting temperatures is probably physiologically restrained – the lipid phases melt at body temperature to allow the tear film to be spread more easily.

Rheometry was used to investigate whether rehydrated porcine mucin can serve as a model for gastric mucus for *in vitro* testing (35). Mucins are the key components of mucus, consisting of a polypeptide backbone with oligosaccharide sidechains, which interpenetrate and form a network in presence of water. Natural mucus was much more elastic than rehydrated mucin, with much stronger resistance to internal structure destruction, probably since the mucin isolation procedure causes such changes in its physicochemical properties that the reconstruction of the initial structure is no longer possible.

Other applications of thermal analysis in medicine

DSC analysis of hair is often used as a quick method to diagnose damage in the hair (and hence the effectiveness of hair repair treatment), but Popescu & Gummer (166) find the claims dubious. Their research provides an example of why the results of the thermal analysis should always be verified by an independent technique, as the “repair” visible from the DSC maximum shift did not reappear in the results by other methods. The two overlapping DSC maxima found for dry hair are denaturation of keratin alpha-helices (~232 °C) and degradation of keratin (~245 °C). Measuring wet hairs allows the separation of these effects, as the denaturation temperature shifts to ~150 °C while the degradation temperature does not change. The research on hair-damaging agents used for hair straightening showed an increase in temperature of degradation of the hair (167), although other characterization methods clearly showed the damage. Maybe the hair-straightening treatment causes additional bonding in the hair which would shift degradation to higher temperatures.

TGA has been extensively used to analyze kidney stones, as covered in a review by Singh and Rai (168), since it can quantify the content of components in the stone, as well as help identify them based on their char-

acteristic degradation temperatures. It is considered the best method to analyze the content of calcium oxalate monohydrate and dihydrate and may provide data that helps determine the age of the stones. Accurate stone analysis is important for correct diagnosis and possible prevention of recurrence (169). But TGA cannot successfully separate components which degrade at similar temperatures and is completely unable to identify or quantify those components which do not lose mass upon heating (168, 169). Of course, the best results are obtained by combining several instrumental techniques.

An interesting application of DSC in medicine was analyzing the composition of collection tubes used in diagnostic procedures, to determine how it may influence the diagnostic results (170). The authors found that the composition varied, as most of the “polypropylene” collection tubes were actually copolymers of polypropylene with polyethylene and sometimes other polymers. The variation in composition led to varying influences on the diagnostic result, most likely due to differences in the adsorption of the biomarkers on the tube surface.

CRITICAL INSIGHTS AND CONCLUSIONS

Thermal analysis methods have been widely used in the fields of biology and medicine for decades. Experiences and molecular models derived from synthetic polymers and inorganic materials are directly transferrable to biological tissues, but researchers should be careful not to be too simplistic in their analysis. Biological samples have very complex compositions, as well as wide diversity within and between the species (37). Macro- and micro-structure (the way in which components are arranged within a tissue) play at least as great a role as the biochemical composition of the tissue (41,45,136). All this makes ascribing certain effects to certain components very difficult, if not impossible. The researchers should be aware of what they are trying to measure and critical of whether the measurement parameters are satisfactory for the purpose, e.g., the influence of a substrate on mechanical properties (121).

Glass transition temperature, for example, can be extremely sensitive to measurement conditions, as well as to the presence of small quantities of plasticizing agents – this can be moisture, but also other small molecules present in the tissue. Thus, care should be taken when trying to explain the experimental data to try and take all known factors into account, and at last to attempt to verify the assumptions on which the explanations rely.

Thermal analysis methods can often be destructive for the samples, especially in the case of TGA. Nevertheless, depending on the temperature range measured, DSC, TMA and DMA may preserve the sample for other investigations, as the mechanical properties are rarely tested to destruction, and DSC may be used to characterize revers-

ible changes such as melting or the glass transition. As small sample sizes are sufficient for DSC and TGA, the destruction of samples during the measurement is rarely an obstacle.

A general problem is that tissues are by necessity regarded in isolation, removed from the living organism (45), so the tissues are usually no longer living and certainly not in their natural state. Selective testing of only certain parts in isolation prevents drawing fuller conclusions (160). Properly separating different tissues can also be difficult, and the variation in separation techniques will certainly influence the results and make them difficult to interpret (134). The influence of preservation treatment on tissue properties should be investigated whenever it is not possible to test the fresh samples (81,143,147). If nothing else, the time from sampling to analysis should be kept the same for all investigated samples in a series.

In some cases, the thermal analysis is performed simply because it is available, without a clear rationale as to what could be learned from it (48, 87, 112, 147). It can also be used merely to confirm what is already known from the experience or other observations (80,110,113,156,161).

Thermal analysis methods give curves with a lot of data, which makes them suitable for mathematical modelling. Care should be taken not to overcomplicate the models: with enough parameters model will be able to fit any data, and any trends will be harder to find (33) due to the compensation effect between the parameters (171). For this reason, it is a good practice to always verify the models on an independent sample or measurement.

Thermal analysis methods are rarely used to characterize the mechanical properties of plants, but they found much wider applications on animal samples, due to the greater flexibility of the methods and small sample sizes needed for the analysis, as well as the ability to measure viscoelastic properties. Mechanical properties of biological samples expectedly show a large scatter (122,127): proper mechanical analysis of synthetic materials also requires a large number of samples, and the diversity in living organisms is comparably greater. A shortcoming of DMA and TMA in comparison with classical mechanical testing methods is a smaller number of measurements per sample, making statistical analysis less likely to find significant correlations or differences (127), even when they are perceptible from the data (143, 152).

Most biological tissues are anisotropic, so variability in properties with the direction of measurement or sampling, as well as across the width or length of the body part or tissue under investigation, should be kept in mind and controlled for (37,105,114,115). Irregular size and shape of the samples can also influence the measurement results, and the researchers are faced with a dilemma of whether to modify the sample as little as possible (44) or to cut it into a suitable shape thus risking making it unrepresentative (116).

Finally, it must be kept in mind that the results of thermal analysis methods can rarely be interpreted on their own and should be verified by an independent technique to confirm the conclusions.

In sum, thermal analysis methods have shown a wide possibility of application in biology and medicine. To obtain the maximum from the data they provide, the researchers should have experience both in the use of the methods and in the investigated tissues or molecules.

Acknowledgements: *The author would like to acknowledge the Croatian microscopy society for its financial and moral support.*

REFERENCES

1. LEVER T, HAINES P, ROUQUEROL J, CHARSLEY E L, VAN ECKEREN P, and BURLETT D J 2014 ICTAC nomenclature of thermal analysis (IUPAC Recommendations 2014). *Pure Appl Chem* 86(4): 545–553. <https://doi.org/10.1515/pac-2012-0609>
2. BROWN M E 2001 *Introduction to Thermal Analysis: Techniques and Applications*, Kluwer Academic Publishers, Dordrecht
3. CLAS S-D, DALTON C R, and HANCOCK B C 1999 Differential scanning calorimetry: applications in drug development. *Pharm Sci Technol Today* 2(8): 311–320. [https://doi.org/10.1016/S1461-5347\(99\)00181-9](https://doi.org/10.1016/S1461-5347(99)00181-9)
4. KNOPP M M, LÖBMANN K, ELDER D P, RADES T, and HOLM R 2016 Recent advances and potential applications of modulated differential scanning calorimetry (mDSC) in drug development. *Eur J Pharm Sci* 87: 164–173. <https://doi.org/10.1016/j.ejps.2015.12.024>
5. CHIAVARO E, Ed, 2014 *Differential Scanning Calorimetry: Applications in Fat and Oil Technology*, CRC Press, Boca Raton
6. FARAH J S, SILVA M C, CRUZ A G, and CALADO V 2018 Differential calorimetry scanning: current background and application in authenticity of dairy products. *Curr Opin Food Sci* 22: 88–94. <https://doi.org/10.1016/j.cofs.2018.02.006>
7. ZHU F 2016 Staling of Chinese steamed bread: Quantification and control. *Trends Food Sci Technol* 55: 118–127. <https://doi.org/10.1016/j.tifs.2016.07.009>
8. NUR AZIRA T and AMIN I 2016 Advances in Differential Scanning Calorimetry for Food Authenticity Testing, In: Downey G (ed) *Advances in Food Authenticity Testing*, Woodhead Publishing, Duxford – Cambridge – Kidlington, p 311.
9. SCHUBRING R 2009 *Differential Scanning Calorimetry*, In: Rehbein H and Oehlenschläger J (eds) *Fishery Products*, Wiley-Blackwell, Oxford, UK, p 173.
10. PIGNATELLO R, Ed, 2013 *Drug-Biomembrane Interaction Studies*, Woodhead Publishing, Oxford – Cambridge – Philadelphia – New Delhi
11. MINETTI C A S A and REMETA D P 2006 Energetics of membrane protein folding and stability. *Arch Biochem Biophys* 453(1): 32–53. <https://doi.org/10.1016/j.abb.2006.03.023>
12. SANCHEZ-RUIZ J M 2010 Protein kinetic stability. *Biophys Chem* 148(1–3): 1–15. <https://doi.org/10.1016/j.bpc.2010.02.004>
13. ENNIFARE E, Ed, 2019 *Microcalorimetry of Biological Molecules: Methods and Protocols*, Springer New York, New York, NY
14. CAÑADAS O and CASALS C 2019 Differential Scanning Calorimetry of Protein–Lipid Interactions, In: Kleinschmidt J H (ed)

- Lipid-Protein Interactions: Methods and Protocols, Springer, New York, NY, p 91.
15. JACOBS M R, GRACE M, BLUMLEIN A, and MCMANUS J J 2019 Differential Scanning Calorimetry to Quantify Heat-Induced Aggregation in Concentrated Protein Solutions, In: McManus J J (ed) Protein Self-Assembly, Springer New York, New York, NY, p 117.
 16. ABOUD R, CHARCOSSET C, and GREIGE-GERGES H 2018 Biophysical methods: Complementary tools to study the influence of human steroid hormones on the liposome membrane properties. *Biochimie* 153: 13–25. <https://doi.org/10.1016/j.biochi.2018.02.005>
 17. BRUYLANTS G, WOUTERS J, and MICHAUX C 2005 Differential scanning calorimetry in life science: Thermodynamics, stability, molecular recognition and application in drug design. *Curr Med Chem* 12(17): 2011–2020. <https://doi.org/10.2174/0929867054546564>
 18. IBARRA-MOLERO B, NAGANATHAN A N, SANCHEZ-RUIZ J M, and MUÑOZ V 2016 Modern Analysis of Protein Folding by Differential Scanning Calorimetry, In: Methods in Enzymology, Elsevier, Cambridge – San Diego – Kidlington – London, p 281
 19. JOHNSON C M 2013 Differential scanning calorimetry as a tool for protein folding and stability. *Arch Biochem Biophys* 531(1–2): 100–109. <https://doi.org/10.1016/j.abb.2012.09.008>
 20. QUINN P J 2012 Lipid–lipid interactions in bilayer membranes: Married couples and casual liaisons. *Prog Lipid Res* 51(3): 179–198. <https://doi.org/10.1016/j.plipres.2012.01.001>
 21. SPINK C H 2008 Differential Scanning Calorimetry, In: Methods in Cell Biology, Elsevier, p 115.
 22. GILL P, MOGHADAM T T, and RANJBAR B 2010 Differential scanning calorimetry techniques: applications in biology and nanoscience. *J Biomol Tech* 21(4): 167–193
 23. CHOWDHRY B 1989 Differential scanning calorimetry: applications in biotechnology. *Trends Biotechnol* 7(1): 11–18. [https://doi.org/10.1016/0167-7799\(89\)90072-3](https://doi.org/10.1016/0167-7799(89)90072-3)
 24. HANSEN L D, RUSSELL D J, and CHOMA C T 2007 From biochemistry to physiology: the calorimetry connection. *Cell Biochem Biophys* 49(2): 125–140. <https://doi.org/10.1007/s12013-007-0049-y>
 25. HESS M, ALLEGRA G, HE J, HORIE K, KIM J-S, MEILLE S V, METANOMSKI V, MOAD G, STEPTO R F T, VERT M, and VOHLÍDAL J 2013 Glossary of terms relating to thermal and thermomechanical properties of polymers (IUPAC Recommendations 2013). *Pure Appl Chem* 85(5): 1017–1046. <https://doi.org/10.1351/PAC-REC-12-03-02>
 26. REH U, KRATZ W, KRAEPELIN G, and ANGEHRN-BETTINAZZI C 1990 Analysis of leaf and needle litter decomposition by differential scanning calorimetry and differential thermogravimetry. *Biol Fertil Soils* 9(2): 188–191. <https://doi.org/10.1007/BF00335806>
 27. NADARAJAN J, MANSOR M, KRISHNAPILLAY B, STAINES H J, BENSON E E, and HARDING K 2008 Applications of differential scanning calorimetry in developing cryopreservation strategies for *Parkia speciosa*, a tropical tree producing recalcitrant seeds. *CryoLetters* 29(2): 95–110.
 28. KAYE A, STEPTO R F T, WORK W J, ALEMÁN J V, and MALKIN A Y 1998 Definition of terms relating to the non-ultimate mechanical properties of polymers (Recommendations 1998). *Pure Appl Chem* 70(3): 701–754. <https://doi.org/10.1351/pac199870030701>
 29. KHAN Md I H and KARIM M A 2017 Cellular water distribution, transport, and its investigation methods for plant-based food material. *Food Res Int* 99: 1–14. <https://doi.org/10.1016/j.foodres.2017.06.037>
 30. HUMPHRIES W T and WILDNAUER R H 1971 Thermomechanical analysis of stratum corneum I. Technique. *J Invest Dermatol* 57(1): 32–37. <https://doi.org/10.1111/1523-1747.ep12292056>
 31. PEREIRA H, CARIDADE S G, FRIAS A M, SILVA-CORREIA J, PEREIRA D R, CENGIZ I F, MANO J F, OLIVEIRA J M, ESPREGUEIRA-MENDES J, and REIS R L 2014 Biomechanical and cellular segmental characterization of human meniscus: building the basis for Tissue Engineering therapies. *Osteoarthritis Cartilage* 22(9): 1271–1281. <https://doi.org/10.1016/j.joca.2014.07.001>
 32. SCALET J M, SPROUSE P A, SCHROEDER J D, DITTMER N, KRAMER K J, KANOST M R, and GEHRKE S H 2022 Temporal changes in the physical and mechanical properties of beetle elytra during maturation. *Acta Biomater* 151: 457–467. <https://doi.org/10.1016/j.actbio.2022.07.059>
 33. CHEN J, ZHAO N, FU N, LI D, WANG L, and CHEN X D 2019 Mechanical properties of hullless barley stem with different moisture contents. *Int J Food Eng* 15(1–2): 20180033. <https://doi.org/10.1515/ijfe-2018-0033>
 34. HINNEN J W, RIXEN D J, KONING O H J, BOCKEL J H VAN, and HAMMING J F 2007 Development of fibrinous thrombus analogue for *in-vitro* abdominal aortic aneurysm studies. *J Biomech* 40(2): 289–295. <https://doi.org/10.1016/j.jbiomech.2006.01.010>
 35. KOČEVAR-NARED J, KRISTL J, and ŠMID-KORBAR J 1997 Comparative rheological investigation of crude gastric mucin and natural gastric mucus. *Biomaterials* 18(9): 677–681. [https://doi.org/10.1016/S0142-9612\(96\)00180-9](https://doi.org/10.1016/S0142-9612(96)00180-9)
 36. ROSENFELD L, CERRETANI C, LEISKE D L, TONEY M F, RADKE C J, and FULLER G G 2013 Structural and rheological properties of meibomian lipid. *Investig Ophthalmology Vis Sci* 54(4): 2720–2732. <https://doi.org/10.1167/iov.12-10987>
 37. ASHADUZZAMAN M, HALE M D, ORMONDROYD G A, and SPEAR M J 2020 Dynamic mechanical analysis of Scots pine and three tropical hardwoods. *Int Wood Prod J* 11(4): 189–203. <https://doi.org/10.1080/20426445.2020.1799910>
 38. WALTERS C, BALLESTEROS D, and VERTUCCI V A 2010 Structural mechanics of seed deterioration: Standing the test of time. *Plant Sci* 179(6): 565–573. <https://doi.org/10.1016/j.plantsci.2010.06.016>
 39. WINDBERGER U, DIBIASI C, LOTZ E M, SCHARBERT G, REINBACHER-KOESTINGER A, IVANOV I, PLOSZCZANSKI L, ANTONOVA N, and LICHTENEGGER H 2020 The effect of hematocrit, fibrinogen concentration and temperature on the kinetics of clot formation of whole blood. *Clin Hemorheol Microcirc* 75(4): 431–445. <https://doi.org/10.3233/CH-190799>
 40. WILLIAMS R J 1994 Methods for determination of glass transitions in seeds. *Ann Bot* 74(5): 525–530. <https://doi.org/10.1006/anbo.1994.1150>
 41. CHUPIN L, SOCCALINGAME L, RIDDER D DE, GINEAU E, MOUILLE G, ARNOULT S, BRANCOURT-HULMEL M, LAPIERRE C, VINCENT L, MIJA A, CORN S, LE MOIGNE N, and NAVARD P 2020 Thermal and dynamic mechanical characterization of miscanthus stem fragments: Effects of genotypes, positions along the stem and their relation with biochemical and structural characteristics. *Ind Crops Prod* 156: 112863. <https://doi.org/10.1016/j.indcrop.2020.112863>
 42. TREVATHAN-TACKETT S M, KELLEWAY J, MACREADDIE P I, BEARDALL J, RALPH P, and BELLGROVE A 2015 Comparison of marine macrophytes for their contributions to blue carbon sequestration. *Ecology* 96(11): 3043–3057. <https://doi.org/10.1890/15-0149.1>

43. METTLER TOLEDO 2016 Thermal Analysis in Practice: Tips and Hints. Mettler-Toledo GmbH, Schwerzenbach
44. BALLESTEROS D and WALTERS C 2019 Solid-state biology and seed longevity: a mechanical analysis of glasses in pea and soybean embryonic axes. *Front Plant Sci* 10: 920. <https://doi.org/10.3389/fpls.2019.00920>
45. NETTI P, D'AMORE A, RONCA D, AMBROSIO L, and NICOLAIS L 1996 Structure-mechanical properties relationship of natural tendons and ligaments. *J Mater Sci Mater Med* 7(9): 525–530. <https://doi.org/10.1007/BF00122175>
46. WU B, ZHAO S, SHI H, LU R, YAN B, MA S, and MARKERT B 2019 Viscoelastic properties of human periodontal ligament: Effects of the loading frequency and location. *Angle Orthod* 89(3): 480–487. <https://doi.org/10.2319/062818-481.1>
47. LOMAKIN J, ARAKANE Y, KRAMER K J, BEEMAN R W, KANOST M R, and GEHRKE S H 2010 Mechanical properties of elytra from *Tribolium castaneum* wild-type and body color mutant strains. *J Insect Physiol* 56(12): 1901–1906. <https://doi.org/10.1016/j.jinsphys.2010.08.012>
48. ALJOUAAA K, TABEIKH H, and ABOUDI M 2017 Characterization of apricot kernel shells (*Prunus armeniaca*) by FTIR spectroscopy, DSC and TGA. *J Indian Acad Wood Sci* 14(2): 127–132. <https://doi.org/10.1007/s13196-017-0197-7>
49. LIU J, PAN Y, YAO C, WANG H, CAO X, and XUE S 2015 Determination of ash content and concomitant acquisition of cell compositions in microalgae via thermogravimetric (TG) analysis. *Algal Res* 12: 149–155. <https://doi.org/10.1016/j.algal.2015.08.018>
50. FENNER R A and LEPHARDT J O 1981 Examination of the thermal decomposition of kraft pine lignin by Fourier transform infrared evolved gas analysis. *J Agric Food Chem* 29(4): 846–849. <https://doi.org/10.1021/jf00106a042>
51. HE W, NAKAO T, YOSHIHARA H, and XUE J S 2011 Treatment of fast-growing poplar with monomers using *in situ* polymerization. Part II: static and dynamic mechanical properties; thermal stability. *For Prod J* 61(2): 121–129. <https://doi.org/10.13073/0015-7473-61.2.121>
52. SHANGGUAN W, CHEN Z, ZHAO J, and SONG X 2018 Thermogravimetric analysis of cork and cork components from *Quercus variabilis*. *Wood Sci Technol* 52(1): 181–192. <https://doi.org/10.1007/s00226-017-0959-9>
53. HAMSTERDANCER 2011 Miscanthus x Gigantheus auf einem Feld bei Firma Sieverdingbeck in NRW. Available at: https://commons.wikimedia.org/wiki/File:Miscanthus_Bestand.JPG (Creative Commons Attribution-Share Alike 3.0)
54. TREVATHAN-TACKETT S M, MACREADIE P I, SANDERMAN J, BALDOCK J, HOWES J M, and RALPH P J 2017 A global assessment of the chemical recalcitrance of seagrass tissues: Implications for long-term carbon sequestration. *Front Plant Sci* 8: 925. <https://doi.org/10.3389/fpls.2017.00925>
55. HAMADA J, PÉTRISSANS A, RUELLE J, MOTHE F, COLIN F, PÉTRISSANS M, and GÉRARDIN P 2018 Thermal stability of *Abies alba* wood according to its radial position and forest management. *Eur J Wood Wood Prod* 76(6): 1669–1676. <https://doi.org/10.1007/s00107-018-1353-5>
56. GARCÍA A V, BELTRÁN SANAHUJA A, and GARRIGÓS SELVA M del C 2013 Characterization and classification of almond cultivars by using spectroscopic and thermal techniques. *J Food Sci* 78(2): C138–C144. <https://doi.org/10.1111/1750-3841.12031>
57. HAMILTON K N, ASHMORE S E, and PRITCHARD H W 2009 Thermal analysis and cryopreservation of seeds of Australian wild *Citrus* species (Rutaceae): *Citrus australasica*, *C. inodora* and *C. garrawayi*. *CryoLetters* 30(3): 268–279
58. MALYSHEV A V, BEIL I, and KREYLING J 2020 Differential Thermal Analysis: A Fast Alternative to Frost Tolerance Measurements. In: Hinch D K and Zuther E (eds) *Plant Cold Acclimation: Methods and Protocols*, Springer US, New York, NY, p 23.
59. HARAŃCZYK H, CASANOVA-KATNY A, OLECH M, and STRZAŁKA K 2017 Dehydration and Freezing Resistance of Lichenized Fungi. In: Shukla V, Kumar S, and Kumar N (eds) *Plant Adaptation Strategies in Changing Environment*, Springer Singapore, Singapore, p 77.
60. DUMONT F, MARECHAL P-A, and GERVAIS P 2006 Involvement of two specific causes of cell mortality in freeze-thaw cycles with freezing to -19°C . *Appl Environ Microbiol* 72(2): 1330–1335. <https://doi.org/10.1128/AEM.72.2.1330-1335.2006>
61. MENON A, FUNNEKOTTER B, KACZMARCZYKA, BUNN E, TURNER S, and MANCERA R L 2012 Cryopreservation of *Lomandra Sonderi* (Asparagaceae) shoot tips using droplet-vitrification. *CryoLetters* 33(4): 259–270.
62. ZHANG J, HUANG B, LU X, VOLK G M, XIN X, YIN G, HE J, and CHEN X 2015 Cryopreservation of *in vitro*-grown shoot tips of Chinese medicinal plant *Atractylodes macrocephala* Koidz. using a droplet-vitrification method. *CryoLetters* 36(3): 195–204.
63. GALE S, BENSON E E, and HARDING K 2013 A life cycle model to enable research of cryostorage recalcitrance in temperate woody species: the case of Sitka spruce (*Picea sitchensis*). *CryoLetters* 34(1): 30–39.
64. TYLEWICZ U, PANARESE V, LAGHI L, ROCCULI P, NOWACKA M, PLACUCCI G, and DALLA ROSA M 2011 NMR and DSC water study during osmotic dehydration of *Actinidia deliciosa* and *Actinidia chinensis* kiwifruit. *Food Biophys* 6(2): 327–333. <https://doi.org/10.1007/s11483-011-9210-7>
65. FERRAZ A, BAEZA J, and DURÁNT N 1991 Softwood biodegradation by an ascomycete *Chrysonilia sitophila* (TFB 27441 strain). *Lett Appl Microbiol* 13(2): 82–86. <https://doi.org/10.1111/j.1472-765X.1991.tb00576.x>
66. ALFREDSEN G, BADER T K, DIBDIAKOVA J, FILBAKK T, BOLLMUS S, and HOFSTETTER K 2012 Thermogravimetric analysis for wood decay characterisation. *Eur J Wood Wood Prod* 70(4): 527–530. <https://doi.org/10.1007/s00107-011-0566-7>
67. MCCARTHY C J, BIRKINSHAW C, PEMBROKE J T, and HALE M 1991 Dynamic mechanical analysis as a technique for the study of fungal degradation of wood. *Biotechnol Tech* 5(6): 493–496. <https://doi.org/10.1007/BF00155502>
68. ORMONDROYD G A, ALFREDSEN G, PRABHAKARAN R T D, CURLING S F, STEFANOWSKI B K, SPEAR M J, and GOBAKKEN L R 2017 Assessment of the use of dynamic mechanical analysis to investigate initial onset of brown rot decay of Scots pine (*Pinus sylvestris* L.). *Int Biodeterior Biodegrad* 120: 1–5. <https://doi.org/10.1016/j.ibiod.2017.02.002>
69. MARVIN H J P, KRECHTING C F, LOO E N VAN, SNIJDERS C H A, NELISSEN L N I H, and DOLSTRA O 1996 Potential of thermal analysis to estimate chemical composition and *in vitro* fermentation characteristics of maize. *J Agric Food Chem* 44(11): 3467–3473. <https://doi.org/10.1021/jf960190q>
70. WINISDORFFER G, MUSSE M, QUELLEC S, BARBACCIA, GALL S L, MARIETTE F, and LAHAYE M 2015 Analysis of the dynamic mechanical properties of apple tissue and relationships with the intracellular water status, gas distribution, histological properties and chemical composition. *Postharvest Biol Technol* 104: 1–16. <https://doi.org/10.1016/j.postharvbio.2015.02.010>
71. HORVATH B, PESZLEN I, PERALTA P, HORVATH L, KASAL B, and LI L 2010 Elastic modulus determination of transgenic aspen using a dynamic mechanical analyzer in static bending mode. *For Prod J* 60(3): 296–300. <https://doi.org/10.13073/0015-7473-60.3.296>

72. LIU Z, JIANG Z, CAI Z, FEI B, YU Y, and LIU X 2012 Dynamic Mechanical Analysis of moso bamboo (*Phyllostachys heterocycla*) at different moisture content. *BioResources* 7(2): 1548–1557. <https://doi.org/10.15376/biores.7.2.1548-1557>
73. CHEN K, LI D, WANG L, ÖZKAN N, CHEN X D, and MAO Z 2007 Dynamic viscoelastic properties of rice kernels studied by dynamic mechanical analyzer. *Int J Food Eng* 3(2). <https://doi.org/10.2202/1556-3758.1227>
74. LIU Y, WANG Y, LV W, LI D, and WANG L 2021 Freeze-thaw and ultrasound pretreatment before microwave combined drying affects drying kinetics, cell structure and quality parameters of *Platycodon grandiflorum*. *Ind Crops Prod* 164: 113391. <https://doi.org/10.1016/j.indcrop.2021.113391>
75. FINNEY E E 1967 Dynamic elastic properties of some fruits during growth and development. *J Agric Eng Res* 12(4): 249–256. [https://doi.org/10.1016/S0021-8634\(67\)80043-X](https://doi.org/10.1016/S0021-8634(67)80043-X)
76. BLAHOVEC J and KOUŘÍM P 2016 Combined mechanical (DMA) and dielectric (DETA) thermal analysis of carrot at temperatures 30–90°C. *J Food Eng* 168: 245–250. <https://doi.org/10.1016/j.jfoodeng.2015.07.044>
77. BLAHOVEC J and KOUŘÍM P 2019 Pulsed electric stimulated changes in potatoes during their cooking: DMA and DETA analysis. *J Food Eng* 240: 183–190. <https://doi.org/10.1016/j.jfoodeng.2018.07.025>
78. ZHAO N, LI B, ZHU Y, LI D, and WANG L 2020 Viscoelastic analysis of oat grain within linear viscoelastic region by using dynamic mechanical analyzer. *Int J Food Eng* 16(4): 20180350. <https://doi.org/10.1515/ijfe-2018-0350>
79. BLANCHET P, KABOORANI A, and BUSTOS C 2016 Understanding effects of drying methods on wood mechanical properties at ultra and cellular levels. *Wood Fiber Sci* 48(2): 117–128.
80. FAHLE S R and THOMASON J C 2008 Measurement of jaw viscoelasticity in newborn and adult lesser spotted dogfish *Scyliorhinus canicula* (L., 1758). *J Fish Biol* 72(6): 1553–1557. <https://doi.org/10.1111/j.1095-8649.2008.01826.x>
81. ABERLE B, JEMMALI R, and DIRKS J-H 2017 Effect of sample treatment on biomechanical properties of insect cuticle. *Arthropod Struct Dev* 46(1): 138–146. <https://doi.org/10.1016/j.asd.2016.08.001>
82. MARCHETTI M D, GÓMEZ P L, YEANNES M I, and GARCIA LOREDO A B 2022 Structure of fish proteins as modified by salting procedures: A rheological and ultrastructural analysis of hake (*Merluccius hubbsi*) fillets. *J Food Sci* 87(3): 1134–1147. <https://doi.org/10.1111/1750-3841.16056>
83. HANS H, MIAO J M, and TRIANTAFYLLOU M S 2014 Mechanical characteristics of harbor seal (*Phoca vitulina*) vibrissae under different circumstances and their implications on its sensing methodology. *Bioinspir Biomim* 9(3): 036013. <https://doi.org/10.1088/1748-3182/9/3/036013>
84. M.BUSCHMANN 2007 Face of *Phoca vitulina*, Germany. Available at: https://commons.wikimedia.org/wiki/File:Phoca_vitulina-face.jpg (Public domain)
85. MARXEN J C, BECKER W, FINKE D, HASSE B, and EPPLE M 2003 Early mineralization in *Biomphalaria glabrata*: microscopic and structural results. *J Molluscan Stud* 69(2): 113–121. <https://doi.org/10.1093/mollus/69.2.113>
86. ALDRED N, WILLS T, WILLIAMS D N, and CLARE A S 2007 Tensile and dynamic mechanical analysis of the distal portion of mussel (*Mytilus edulis*) byssal threads. *J R Soc Interface* 4(17): 1159–1167. <https://doi.org/10.1098/rsif.2007.1026>
87. PRASONG S, YAOWALAK S, and WILAIWAN S 2009 Characteristics of silk fiber with and without sericin component: A comparison between *Bombyx mori* and *Philosamia ricini* silks. *Pak J Biol Sci* 12(11): 872–876. <https://doi.org/10.3923/pjbs.2009.872.876>
88. TESHOME A, RAINA S K, and VOLLRATH F 2014 Structure and properties of silk from the African wild silkworm <i>Gonometta postica</i> reared indoors. *J Insect Sci* 14(36): 1–9. <https://doi.org/10.1673/031.014.36>
89. PORTER D, VOLLRATH F, and SHAO Z 2005 Predicting the mechanical properties of spider silk as a model nanostructured polymer. *Eur Phys J E* 16(2): 199–206. <https://doi.org/10.1140/epje/e2005-00021-2>
90. BLACKLEDGE T A, SWINDEMAN J E, and HAYASHI C Y 2005 Quasistatic and continuous dynamic characterization of the mechanical properties of silk from the cobweb of the black widow spider *Latrodectus hesperus*. *J Exp Biol* 208(10): 1937–1949. <https://doi.org/10.1242/jeb.01597>
91. MOTOKAWA T and TSUCHI A 2003 Dynamic mechanical properties of body-wall dermis in various mechanical states and their implications for the behavior of sea cucumbers. *Biol Bull* 205(3): 261–275. <https://doi.org/10.2307/1543290>
92. MOTOKAWA T 2011 Mechanical mutability in connective tissue of starfish body wall. *Biol Bull* 221(3): 280–289. <https://doi.org/10.1086/BBLv221n3p280>
93. ALPAS H, LEE J, BOZOGLU F, and KALETUNÇ G 2003 Evaluation of high hydrostatic pressure sensitivity of *Staphylococcus aureus* and *Escherichia coli* O157:H7 by differential scanning calorimetry. *Int J Food Microbiol* 87(3): 229–237. [https://doi.org/10.1016/S0168-1605\(03\)00066-7](https://doi.org/10.1016/S0168-1605(03)00066-7)
94. MILES C A, MACKEY B M, and PARSONS S E 1986 Differential scanning calorimetry of bacteria. *Microbiology* 132(4): 939–952. <https://doi.org/10.1099/00221287-132-4-939>
95. ANDERSON W A, HEDGES N D, JONES M V, and COLE M B 1991 Thermal inactivation of *Listeria monocytogenes* studied by differential scanning calorimetry. *J Gen Microbiol* 137(6): 1419–1424. <https://doi.org/10.1099/00221287-137-6-1419>
96. MILEK I, ČRNIGOJ M, ULRIH N P, and KALETUNÇ G 2007 *In vivo* characterization of thermal stabilities of *Aeropyrum pernix* cellular components by differential scanning calorimetry. *Can J Microbiol* 53(9): 1038–1045. <https://doi.org/10.1139/W07-069>
97. LEE J and KALETUNÇ G 2002 Evaluation of the heat inactivation of *Escherichia coli* and *Lactobacillus plantarum* by differential scanning calorimetry. *Appl Environ Microbiol* 68(11): 5379–5386. <https://doi.org/10.1128/AEM.68.11.5379-5386.2002>
98. LEE J and KALETUNÇ G 2002 Calorimetric determination of inactivation parameters of micro-organisms. *J Appl Microbiol* 93(1): 178–189. <https://doi.org/10.1046/j.1365-2672.2002.01677.x>
99. STEPHENS P J and JONES M V 1993 Reduced ribosomal thermal denaturation in *Listeria monocytogenes* following osmotic and heat shocks. *FEMS Microbiol Lett* 106(2): 177–182. <https://doi.org/10.1111/j.1574-6968.1993.tb05955.x>
100. BELLIVEAU B H, BEAMAN T C, PANKRATZ H S, and GERHARDT P 1992 Heat killing of bacterial spores analyzed by differential scanning calorimetry. *J Bacteriol* 174(13): 4463–4474. <https://doi.org/10.1128/jb.174.13.4463-4474.1992>
101. STECCHINI M L, DEL TORRE M, VENIR E, MORETTIN A, FURLAN P, and MALTINI E 2006 Glassy state in *Bacillus subtilis* spores analyzed by differential scanning calorimetry. *Int J Food Microbiol* 106(3): 286–290. <https://doi.org/10.1016/j.jfoodmicro.2005.06.028>
102. LEUSCHNER R G K and LILLFORD P J 2003 Thermal properties of bacterial spores and biopolymers. *Int J Food Microbiol* 80(2): 131–143. [https://doi.org/10.1016/S0168-1605\(02\)00139-3](https://doi.org/10.1016/S0168-1605(02)00139-3)
103. ILLMER P, ERLEBACH C, and SCHINNER F 1999 A practicable and accurate method to differentiate between intra- and

- extracellular water of microbial cells. *FEMS Microbiol Lett* 178(1): 135–139.
<https://doi.org/10.1111/j.1574-6968.1999.tb13769.x>
104. URIBELARREA J L, PACAUD S, and GOMA G 1985 New method for measuring the cell water content by thermogravimetry. *Biotechnol Lett* 7(2): 75–80.
<https://doi.org/10.1007/BF01026672>
 105. APTER J and MASON P 1971 Dynamic mechanical properties of mammalian ureteral muscle. *Am J Physiol-Leg Content* 221(1): 266–272. <https://doi.org/10.1152/ajplegacy.1971.221.1.266>
 106. FITZGERALD E R 1975 Dynamic mechanical measurements during the life to death transition in animal tissues. *Biorheology* 12(6): 397–408. <https://doi.org/10.3233/BIR-1975-12611>
 107. CHATELIN S, OUDRY J, PÉRICHON N, SANDRIN L, ALLEMANN P, SOLER L, and WILLINGER R 2011 *In vivo* liver tissue mechanical properties by transient elastography: Comparison with dynamic mechanical analysis. *Biorheology* 48(2): 75–88. <https://doi.org/10.3233/BIR-2011-0584>
 108. BARTLETT R D, ELEFThERiADOU D, EVANS R, CHOI D, and PHILLIPS J B 2020 Mechanical properties of the spinal cord and brain: Comparison with clinical-grade biomaterials for tissue engineering and regenerative medicine. *Biomaterials* 258: 120303. <https://doi.org/10.1016/j.biomaterials.2020.120303>
 109. SCHULZA, WAHL S, RICKMANN A, LUDWIG J, STANZEL B V, BRIESEN H VON, and SZURMAN P 2019 Age-related loss of human vitreal viscoelasticity. *Transl Vis Sci Technol* 8(3): 56. <https://doi.org/10.1167/tvst.8.3.56>
 110. WEEBER H A, ECKERT G, SOERGEL F, MEYER C H, PECHHOLD W, and HEIJDE R G L VAN DER 2005 Dynamic mechanical properties of human lenses. *Exp Eye Res* 80(3): 425–434. <https://doi.org/10.1016/j.exer.2004.10.010>
 111. LIU J, KIM E K, NIA, KIM Y-R, ZHENG F, LEE B S, and KIM D-G 2021 Multiscale characterization of ovariectomized rat femur. *J Biomech* 122: 110462.
<https://doi.org/10.1016/j.jbiomech.2021.110462>
 112. FRIIS S J, HANSEN T S, POULSEN M, GREGERSEN H, and NYGAARD J V 2022 Dynamic viscoelastic properties of porcine gastric tissue: Effects of loading frequency, region and direction. *J Biomech* 143: 111302.
<https://doi.org/10.1016/j.jbiomech.2022.111302>
 113. ZERNICKE R F, VAILAS A C, SHAW S R, BOGEY R A, HART T J, and MATSUDA J 1986 Heterogeneous mechanical response of rat knee menisci to thermomechanical stress. *Am J Physiol-Regul Integr Comp Physiol* 250(1): R65–R70.
<https://doi.org/10.1152/ajpregu.1986.250.1.R65>
 114. NORBERG C, FILIPPONE G, ANDREOPOULOS F, BEST T M, BARAGA M, JACKSON A R, and TRAVASCIO F 2021 Viscoelastic and equilibrium shear properties of human meniscus: Relationships with tissue structure and composition. *J Biomech* 120: 110343. <https://doi.org/10.1016/j.jbiomech.2021.110343>
 115. FELL N L A, LAWLESS B M, COX S C, COOKE M E, EISENSTEIN N M, SHEPHERD D E T, and ESPINO D M 2019 The role of subchondral bone, and its histomorphology, on the dynamic viscoelasticity of cartilage, bone and osteochondral cores. *Osteoarthritis Cartilage* 27(3): 535–543.
<https://doi.org/10.1016/j.joca.2018.12.006>
 116. ZHU H, BHATIA S, and CHAUHAN A 2007 Dynamic mechanical properties of porcine lacrimal canaliculus. *Curr Eye Res* 32(10): 829–835. <https://doi.org/10.1080/02713680701598503>
 117. AOBA T, YOSHIOKA C, OGAWA Y, and YAGI T 1978 A study of the mineral phase of cementifying fibroma. *J Oral Pathol Med* 7(3): 156–161.
<https://doi.org/10.1111/j.1600-0714.1978.tb01591.x>
 118. MOUNTCASTLE S E, ALLEN P, MELLORS B O L, LAWLESS B M, COOKE M E, LAVECCHIA C E, FELL N L A, ESPINO D M, JONES S W, and COX S C 2019 Dynamic viscoelastic characterisation of human osteochondral tissue: understanding the effect of the cartilage-bone interface. *BMC Musculoskelet Disord* 20(1): 575.
<https://doi.org/10.1186/s12891-019-2959-4>
 119. TEMPLE D K, CEDERLUND A A, LAWLESS B M, ASPDEN R M, and ESPINO D M 2016 Viscoelastic properties of human and bovine articular cartilage: a comparison of frequency-dependent trends. *BMC Musculoskelet Disord* 17(1): 419.
<https://doi.org/10.1186/s12891-016-1279-1>
 120. ESPINO D M, SHEPHERD D E, and HUKINS D W 2014 Viscoelastic properties of bovine knee joint articular cartilage: dependency on thickness and loading frequency. *BMC Musculoskelet Disord* 15(1): 205.
<https://doi.org/10.1186/1471-2474-15-205>
 121. CROLLA J P, LAWLESS B M, CEDERLUND A A, ASPDEN R M, and ESPINO D M 2022 Analysis of hydration and subchondral bone density on the viscoelastic properties of bovine articular cartilage. *BMC Musculoskelet Disord* 23(1): 228.
<https://doi.org/10.1186/s12891-022-05169-0>
 122. GUEDES R M, SIMÕES J A, and MORAIS J L 2006 Viscoelastic behaviour and failure of bovine cancellous bone under constant strain rate. *J Biomech* 39(1): 49–60.
<https://doi.org/10.1016/j.jbiomech.2004.11.005>
 123. LAMBRI O A, PÉREZ-LANDEZÁBAL J I, BONIFACICH F G, RECARTE V, LAMBRI M L, ZELADA G I, TARDITTI F, and GARGICEVICH D 2014 Damping micromechanisms for bones above room temperature. *J Biomim Biomater Tissue Eng* 19: 87–98.
<https://doi.org/10.4028/www.scientific.net/JBBTE.19.87>
 124. MAKY.OREL 2019 Femur (caput femoris) - bone structure detail (vertical cut) 2. Available at:
[https://commons.wikimedia.org/wiki/File:Femur_\(caput_femoris\)_-_bone_structure_detail_\(vertical_cut\)_2.jpg](https://commons.wikimedia.org/wiki/File:Femur_(caput_femoris)_-_bone_structure_detail_(vertical_cut)_2.jpg) (Public domain)
 125. PINEDA-GOMEZ P, HERNÁNDEZ-BECERRA E, ROJAS-MOLINA I, ROSALES-RIVERA A, and RODRÍGUEZ-GARCÍA M E 2019 The effect of calcium deficiency on bone properties in growing rats. *Curr Nutr Food Sci* 15(5): 467–475.
<https://doi.org/10.2174/1573401314666180919142102>
 126. LES C M, VANCE J L, CHRISTOPHERSON G T, TURNER A S, DIVINE G W, and FYHRIE D P 2005 Long-term ovariectomy decreases ovine compact bone viscoelasticity. *J Orthop Res* 23(4): 869–876. <https://doi.org/10.1016/j.orthres.2004.12.001>
 127. LEHMANN T P, WOJTKÓW M, PRUSZYŃSKA-OSZMAŁEK E, KOŁODZIEJSKI P, PEZOWICZ C, TRZASKOWSKA A, MIELCAREK S, SZYBOWICZ M, NOWICKA A B, NOWICKI M, MISTERSKA E, IWAŃCZYK-SKALSKA E, JAGODZIŃSKI P, and GŁOWACKI M 2021 Trabecular bone remodelling in the femur of C57BL/6J mice treated with diclofenac in combination with treadmill exercise. *Acta Bioeng Biomech* 23(3): 3–11.
<https://doi.org/10.37190/ABB-01851-2021-01>
 128. BAUM O I, SOSHNIKOVA Y M, SOBOL E N, KORNEYCHUK A Ya, OBREZKOVA M V, SVISTUSHKIN V M, TIMOFEEVA O K, and LUNIN V V 2011 Laser reshaping of costal cartilage for transplantation. *Lasers Surg Med* 43(6): 511–515. <https://doi.org/10.1002/lsm.21077>
 129. CHAE Y, AGUILAR G, LAVERNIA E J, and WONG B J F 2003 Characterization of temperature dependent mechanical behavior of cartilage. *Lasers Surg Med* 32(4): 271–278.
<https://doi.org/10.1002/lsm.10167>

130. YU X, CHEN G, and ZHANG S 2013 A refinement to the liquidus-tracking method for vitreous preservation of articular cartilage. *CryoLetters* 34(3): 267–276.
131. HOLAGER J 1970 Thermogravimetric examination of enamel and dentin. *J Dent Res* 49(3): 546–548. <https://doi.org/10.1177/00220345700490031301>
132. LIM J J and LIBOFF A R 1972 Thermogravimetric analysis of dentin. *J Dent Res* 51(2): 509–514. <https://doi.org/10.1177/00220345720510024401>
133. ELFERSI S, GRÉGOIRE G, and SHARROCK P 2002 Characterization of sound human dentin particles of sub-millimeter size. *Dent Mater* 18(7): 529–534. [https://doi.org/10.1016/S0109-5641\(01\)00085-9](https://doi.org/10.1016/S0109-5641(01)00085-9)
134. LARMAS M A, HÄYRYNEN H, and LAJUNEN L H 1993 Thermogravimetric studies on sound and carious human enamel and dentin as well as hydroxyapatite. *Eur J Oral Sci* 101(4): 185–191. <https://doi.org/10.1111/j.1600-0722.1993.tb01102.x>
135. KEREBEL B, DACULSI G, MENANTEAU J, and KEREBEL L M 1981 The inorganic phase in *Dentinogenesis imperfecta*. *J Dent Res* 60(9): 1655–1660. <https://doi.org/10.1177/00220345810600090401>
136. TERUEL J de D, ALCOLEA A, HERNÁNDEZ A, and RUIZ A J O 2015 Comparison of chemical composition of enamel and dentine in human, bovine, porcine and ovine teeth. *Arch Oral Biol* 60(5): 768–775. <https://doi.org/10.1016/j.archoralbio.2015.01.014>
137. HUMPHRIES W T and WILDNAUER R H 1972 Thermomechanical analysis of stratum corneum II. Application. *J Invest Dermatol* 58(1): 9–13. <https://doi.org/10.1111/1523-1747.ep13077184>
138. MILLER D L and WILDNAUER R H 1977 Thermoanalytical probes for the analysis of physical properties of stratum corneum. *J Invest Dermatol* 69(3): 287–289. <https://doi.org/10.1111/1523-1747.ep12507507>
139. WILKES G L and WILDNAUER R H 1973 Structure-property relationships of the stratum corneum of human and neonatal rat II. Dynamic mechanical studies. *Biochim Biophys Acta BBA - Gen Subj* 304(2): 276–289. [https://doi.org/10.1016/0304-4165\(73\)90245-6](https://doi.org/10.1016/0304-4165(73)90245-6)
140. MELLING M, PFEILER W, KARIMIAN-TEHERANI D, SCHNALLINGER M, SOBAL G, ZANGERLE C, and MENZEL E J 2000 Differential scanning calorimetry, biochemical, and biomechanical analysis of human skin from individuals with diabetes mellitus. *Anat Rec* 259(3): 327–333. [https://doi.org/10.1002/1097-0185\(20000701\)259:3<327::AID-AR90>3.0.CO;2-G](https://doi.org/10.1002/1097-0185(20000701)259:3<327::AID-AR90>3.0.CO;2-G)
141. MARCHESSEAU S, HEIMANN T, CHATELIN S, WILLINGER R, and DELINGETTE H 2010 Fast porous visco-hyperelastic soft tissue model for surgery simulation: Application to liver surgery. *Prog Biophys Mol Biol* 103(2): 185–196. <https://doi.org/10.1016/j.pbiomolbio.2010.09.005>
142. KHOSRAVIA, BANI M S, BAHREINIZAD H, and KARIMI A 2017 Viscoelastic properties of the autologous bypass grafts: A comparative study among the small saphenous vein and internal thoracic artery. *Artery Res* 19(C): 65–71. <https://doi.org/10.1016/j.artres.2017.06.007>
143. SINGH D, BOAKYE-YIADOM S, and CRONIN D S 2019 Comparison of porcine brain mechanical properties to potential tissue simulant materials in quasi-static and sinusoidal compression. *J Biomech* 92: 84–91. <https://doi.org/10.1016/j.jbiomech.2019.05.033>
144. WORTHINGTON K S, WILEY L A, BARTLETT A M, STONE E M, MULLINS R F, SALEM A K, GUYMON C A, and TUCKER B A 2014 Mechanical properties of murine and porcine ocular tissues in compression. *Exp Eye Res* 121: 194–199. <https://doi.org/10.1016/j.exer.2014.02.020>
145. FALLENSTEIN G T, HULCE V D, and MELVIN J W 1969 Dynamic mechanical properties of human brain tissue. *J Biomech* 2(3): 217–226. [https://doi.org/10.1016/0021-9290\(69\)90079-7](https://doi.org/10.1016/0021-9290(69)90079-7)
146. GÖTZ M E, FREYBERGER A, HAUER E, BURGER R, SOFIC E, GSELL W, HECKERS S, JELLINGER K, HEBENSTREIT G, FRÖLICH L, BECKMANN H, and RIEDERER P 1992 Susceptibility of brains from patients with Alzheimer's disease to oxygen-stimulated lipid peroxidation and differential scanning calorimetry. *Dement Geriatr Cogn Disord* 3(4): 213–222. <https://doi.org/10.1159/000107020>
147. BARBERIO C G, CHAUDHRY T, POWER D M, TAN S, LAWLESS B M, ESPINO D M, and WILTON J C 2019 Towards viscoelastic characterisation of the human ulnar nerve: An early assessment using embalmed cadavers. *Med Eng Phys* 64: 15–22. <https://doi.org/10.1016/j.medengphy.2018.12.009>
148. PI Z, WANG M, LIN H, GUO Y, CHEN S, DIAO X, XIA H, LIU G, ZENG J, ZHANG X, and CHEN X 2021 Viscoelasticity measured by shear wave elastography in a rat model of nonalcoholic fatty liver disease: comparison with dynamic mechanical analysis. *Biomed Eng OnLine* 20(1): 45. <https://doi.org/10.1186/s12938-021-00879-3>
149. ZHANG X, GAO X, ZHANG P, GUO Y, LIN H, DIAO X, LIU Y, DONG C, HU Y, CHEN S, and CHEN X 2017 Dynamic mechanical analysis to assess viscoelasticity of liver tissue in a rat model of nonalcoholic fatty liver disease. *Med Eng Phys* 44: 79–86. <https://doi.org/10.1016/j.medengphy.2017.02.014>
150. LEONG S S, WONG J H D, MD SHAH M N, VIJAYANANTHAN A, JALALONMUHALI M, MOHD SHARIF N H, ABAS N K, and NG K H 2020 Stiffness and anisotropy effect on shear wave elastography: A phantom and *in vivo* renal study. *Ultrasound Med Biol* 46(1): 34–45. <https://doi.org/10.1016/j.ultrasmedbio.2019.08.011>
151. BETTELHEIM F A, CHRISTIAN S, and LEE L-K 1982 Differential scanning calorimetric measurements on human lenses. *Curr Eye Res* 2(12): 803–808. <https://doi.org/10.3109/02713688209020015>
152. BETTELHEIM F A and MOFUNANYA A 2001 Synergetic response to pressure in bovine and rhesus monkey vitreous. *Exp Eye Res* 73(1): 133–136. <https://doi.org/10.1006/exer.2001.1021>
153. LUNDGREN C H, WILLIAMS T R, and NUNNARI J M 1986 Determination of the state and content of water in normal avian, fish, porcine, bovine, and human lenses as studied by differential scanning calorimetry. *Ophthalmic Res* 18(2): 90–97. <https://doi.org/10.1159/000265421>
154. NIH IMAGE GALLERY 2016 A hypermature age-related cortico-nuclear cataract with a brunescens (brown) nucleus. Available at: [https://commons.wikimedia.org/wiki/File:Cataract_\(28464844371\).png](https://commons.wikimedia.org/wiki/File:Cataract_(28464844371).png) (Public domain)
155. HEYS K R and TRUSCOTT R J W 2008 The stiffness of human cataract lenses is a function of both age and the type of cataract. *Exp Eye Res* 86(4): 701–703. <https://doi.org/10.1016/j.exer.2007.12.009>
156. HEYS K R, CRAM S L, and WILLIS TRUSCOTT R J 2004 Massive increase in the stiffness of the human lens nucleus with age: the basis for presbyopia? *Mol Vis* 10: 956–963.
157. SCHACHAR R A 2005 Comment on 'Dynamic mechanical properties of human lenses' by H. A. Weeber et al. [*Exp. Eye Res.* 80 (2005) 425–434]. *Exp Eye Res* 81(2): 236. <https://doi.org/10.1016/j.exer.2005.03.016>
158. TOKITA M, FUJIYA Y, and HIKICHI K 1984 Dynamic viscoelasticity of bovine vitreous body. *Biorheology* 21(6): 751–756. <https://doi.org/10.3233/BIR-1984-21602>

159. KRASIŃSKI Z, BISKUPSKI P, DZIECIUCHOWICZ Ł, KACZMAREK E, KRASIŃSKA B, STANISZEWSKI R, PAWLACZYK K, STANISIĆ M, MAJEWSKI P, and MAJEWSKI W 2010 The influence of elastic components of the venous wall on the biomechanical properties of different veins used for arterial reconstruction. *Eur J Vasc Endovasc Surg* 40(2): 224–229. <https://doi.org/10.1016/j.ejvs.2010.04.008>
160. SMITH G E, BARNES R, FAGAN M, and CHETTER I C 2016 The impact of vein mechanical compliance on arteriovenous fistula outcomes. *Ann Vasc Surg* 32: 9–14. <https://doi.org/10.1016/j.avsg.2015.11.002>
161. XU Y, HUA T-C, SUN D-W, ZHOU G-Y, and XU F 2007 Effects of freezing rates and dimethyl sulfoxide concentrations on thermal expansion of rabbit aorta during freezing phase change as measured by thermo mechanical analysis. *J Biomech* 40(14): 3201–3206. <https://doi.org/10.1016/j.jbiomech.2007.04.010>
162. NUNES J M, FILLIS T, PAGE M J, VENTER C, LANCRY O, KELL D B, WINDBERGER U, and PRETORIUS E 2020 Gingipain R1 and lipopolysaccharide from *Porphyromonas gingivalis* have major effects on blood clot morphology and mechanics. *Front Immunol* 11: 1551. <https://doi.org/10.3389/fimmu.2020.01551>
163. NAIR P M, PIDCOKE H F, CAP A P, and RAMASUBRAMANIAN A K 2014 Effect of cold storage on shear-induced platelet aggregation and clot strength. *J Trauma Acute Care Surg* 77(3): S88–S93. <https://doi.org/10.1097/TA.0000000000000327>
164. LEE R T, GRODZINSKY A J, FRANK E H, KAMM R D, and SCHOEN F J 1991 Structure-dependent dynamic mechanical behavior of fibrous caps from human atherosclerotic plaques. *Circulation* 83(5): 1764–1770. <https://doi.org/10.1161/01.CIR.83.5.1764>
165. CHAGOVETZ A A, JENSEN R L, RECHT L, GLANTZ M, and CHAGOVETZ A M 2011 Preliminary use of differential scanning calorimetry of cerebrospinal fluid for the diagnosis of glioblastoma multiforme. *J Neurooncol* 105(3): 499–506. <https://doi.org/10.1007/s11060-011-0630-5>
166. POPESCU C and GUMMER C 2016 DSC of human hair: a tool for claim support or incorrect data analysis? *Int J Cosmet Sci* 38(5): 433–439. <https://doi.org/10.1111/ics.12306>
167. LEITE M G A and MAIA CAMPOS P M B G 2017 Mechanical characterization of curly hair: Influence of the use of nonconventional hair straightening treatments. *Skin Res Technol* 23(4): 539–544. <https://doi.org/10.1111/srt.12368>
168. SINGH V K and RAI P K 2014 Kidney stone analysis techniques and the role of major and trace elements on their pathogenesis: a review. *Biophys Rev* 6(3–4): 291–310. <https://doi.org/10.1007/s12551-014-0144-4>
169. KASIDAS G P, SAMUEL C T, and WEIR T B 2004 Renal stone analysis: why and how? *Ann Clin Biochem Int J Lab Med* 41(2): 91–97. <https://doi.org/10.1258/000456304322879962>
170. PERRET-LIAUDET A, PELPEL M, THOLANCE Y, DUMONT B, VANDERSTICHELE H, ZORZI W, ELMOUALIJ B, SCHRAEN S, MOREAUD O, GABELLE A, THOUVENOT E, THOMAS-ANTERION C, TOUCHON J, KROLAK-SALMON P, KOVACS G G, COUDREUSE A, QUADRIO I, and LEHMANN S 2012 Risk of Alzheimer's disease biological misdiagnosis linked to cerebrospinal collection tubes. *J Alzheimers Dis* 31(1): 13–20. <https://doi.org/10.3233/JAD-2012-120361>
171. VYAZOVKIN S and WIGHT C A 1997 Isothermal and Non-isothermal Reaction Kinetics in Solids: In Search of Ways toward Consensus. *J Phys Chem A* 101(44): 8279–8284. <https://doi.org/10.1021/jp971889h>